TAMPEREEN TEKNILLINEN YLIOPISTO
TAMPERE UNIVERSITY OF TECHNOLOGY

Matti Happonen

Particle and NO_x Emissions from a HVO-Fueled Diesel Engine

Julkaisu 1078 • Publication 1078

Tampere 2012

Tampereen teknillinen yliopisto. Julkaisu 1078
Tampere University of Technology. Publication 1078

Matti Happonen

Particle and NO_x Emissions from a HVO-Fueled Diesel Engine

Thesis for the degree of Doctor of Science in Technology to be presented with due permission for public examination and criticism in Sähkötalo Building, Auditorium S4, at Tampere University of Technology, on the 26th of October 2012, at 12 noon.

Tampereen teknillinen yliopisto - Tampere University of Technology
Tampere 2012

Doctoral candidate: Matti Happonen, M.Sc.
Aerosol Physics Laboratory
Department of Physics
Tampere University of Technology
Present address:
Ecocat Oy, Vihtavuori

Supervisors: Annele Virtanen, assoc. prof.
Aerosol Physics Laboratory
Department of Physics
Tampere University of Technology
Present address:
Department of Applied Physics
University of Eastern Finland, Kuopio

Jorma Keskinen, prof.
Aerosol Physics Laboratory
Department of Physics
Tampere University of Technology

Pre-examiners: Miroslaw L. Wyszynski, prof.
School of Mechanical Engineering
University of Birmingham

Erik Swietlicki, prof.
Division of Nuclear Physics
Department of Physics
Lund University

Opponent: Heejung Jung, assoc. prof.
Department of Mechanical Engineering and CE-CERT
University of California, Riverside

ISBN 978-952-15-2921-4 (printed)
ISBN 978-952-15-2935-1 (PDF)
ISSN 1459-2045

Abstract

Concerns about oil price, the strengthening climate change and traffic related health effects are all reasons which have promoted the research of renewable fuels. One renewable fuel candidate is diesel consisting of hydrotreated vegetable oils (HVO). The fuel is essentially paraffinic, has high cetane number (>80) and contains practically no oxygen, aromatics or sulphur. Furthermore, HVO fuel can be produced from various feedstocks including palm, soybean and rapeseed oils as well as animal fats. HVO has also been observed to reduce all regulated engine exhaust emissions compared to conventional diesel fuel.

In this thesis, the effect of HVO fuel on engine exhaust emissions has been studied further. The thesis is roughly divided into two parts. The first part explores the emission reductions associated with the fuel and studies techniques which could be applied to achieve further emission reductions. One of the studied techniques was adjusting engine settings to better suit HVO fuel. The settings chosen for adjustments were injection pressure, injection timing, the amount of EGR and the timing of inlet valve closing (with constant inlet air mass flow, i.e. Miller timing). The engine adjustments were also successfully targeted to reduce either NO_x or particulate emissions or both. The other applied emission reduction technique was the addition of oxygenate to HVO fuel. The chosen oxygenate was di-n-pentyl ether (DNPE), and tested fuel blend included 20 wt-% DNPE and 80 wt-% HVO. Thus, the oxygen content of the resulting blend was 2 wt-%. Reductions of over 25 % were observed in particulate emissions with the blend compared to pure HVO while NO_x emissions altered under 5 %.

On the second part of this thesis, the effect of the studied fuels on chosen surface properties of exhaust particles were studied using tandem differential mobility analyzer (TDMA) techniques and transmission electron microscopy (TEM). The studied surface properties were oxidizability and hygroscopicity. The oxidation properties were compared between soot particles emitted with HVO and with conventional diesel. The effects of fuel on hygroscopicity, on the other hand, were compared between HVO and oxygenated HVO fuel. In general, no considerable differences were observed in the exhaust particle surface properties due to the change of fuel.

II

Preface

The work of this thesis has been conducted in the Aerosol Physics Laboratory of the Department of Physics at Tampere University of Technology during the years 2009–2012. I want to thank my supervisor Doc. Annele Virtanen for her guidance and support. Also, I would like to thank professor Jorma Keskinen, for his advises and, especially, for the opportunity to work in the Aerosol Physics Laboratory in the first place.

No single researcher, nor even an institute in this case, can take all the credit for the work presented in this thesis. Therefore, I would like to express my sincere thanks to the group of professor Martti Larmi from Aalto University, especially Kalle Lehto and Teemu Sarjovaara, for operating the engine bench, to Maria Messing and Reine Wallenberg (Lund University) for HRTEM and EELS analyses and to Timo Murtonen and Päivi Aakko-Saksa (VTT) for PM measurements and chemical expertise. It has been a real pleasure to work with you.

The same is valid also for the whole OQ group. Especially, I would like to thank Juha Heikkilä, with whom I have written most of the papers of this thesis, Tero Lähde and Topi Rönkkö, who guided me to the world of engine emissions and TDMA techniques, and Antti Rostedt, without whom the HTDMA would not have been built in time for the oxygenate measurements. Also, I would like to thank my roommates at work, Juha Harra and Heino Kuuluvainen, for creating this extraordinary atmosphere in which publishing bad pictures was not an option but, due to the standards set high, still hard to avoid.

I acknowledge professor Miroslaw L. Wyszynski and professor Erik Swietlicki for the pre-examination of the thesis, as well as the project funding from Tekes – the Finnish Funding Agency for Technology and Innovation and Neste Oil Oyj. The personal financial support granted by Maj and Thor Nessling foundation, Kauko Haikarainen foundation, Finnish Foundation for Technology Promotion and Henry Ford foundation are also sincerely acknowledged.

There are also people who have supported me to go on, not just through this thesis work, but throughout all my education. I am talking about my parents and my sister of course. Eila, Terho and Mari, you own my deepest thanks. Finally, I would like to thank my wife Pirjo for her love and for the patience she has shown over this project. I also appreciate her for kicking me off the bed to work at mornings. As for my daughter Veera, I think that I can safely say that you have no idea how much your presence has motivated me to finish the thesis in the schedule, so to speak.

List of included publications

This thesis is a compound thesis consisting of an introductory review and the following four publications. The publications are cited in the introductory review according to their numbering presented below.

Paper 1 **Juha Heikkilä, Matti Happonen, Timo Murtonen, Kalle Lehto, Teemu Sarjovaara, Martti Larmi, Jorma Keskinen, Annele Virtanen**, "Effect of Miller timing on particulate emissions of a HVO fueled research engine", *Journal of the Air and Waste Management Association*, accepted in June 2012. DOI:10.1080/10962247.2012.708383.

Paper 2 **Matti Happonen, Juha Heikkilä, Timo Murtonen, Kalle Lehto, Teemu Sarjovaara, Martti Larmi, Jorma Keskinen, Annele Virtanen**, "Reductions in particulate and NO_x emissions by diesel engine parameter adjustments with HVO fuel", *Environmental Science & Technology* **46**, 2012, pp. 6198–6204.

Paper 3 **Matti Happonen, Juha Heikkilä, Päivi Aakko-Saksa, Timo Murtonen, Kalle Lehto, Teemu Sarjovaara, Antti Rostedt, Martti Larmi, Jorma Keskinen, Annele Virtanen**, "Diesel exhaust emissions and particle hygroscopicity with HVO fuel-oxygenate blend", *Fuel*, accepted in September 2012. DOI:10.1016/j.fuel.2012.09.006.

Paper 4 **Matti Happonen, Tero Lähde, Maria E. Messing, Teemu Sarjovaara, Martti Larmi, L. Reine Wallenberg, Annele Virtanen, Jorma Keskinen**, "The comparison of particle oxidation and surface structure of diesel soot particles between fossil fuel and novel renewable diesel fuel", *Fuel* **89**, 2010, pp. 4008–4013.

Author's contributions to the publications

Paper 1: I planned and conducted particle size distribution measurements jointly with Juha Heikkilä. Further, I participated in deciding the contents of the paper and I had a minor contribution in the writing of the paper.

Paper 2: I planned and conducted particle size distribution measurements jointly with Juha Heikkilä. In addition, I conducted the data-analysis, decided the contents of the paper and, with minor contribution from other authors, wrote the paper.

Paper 3: I planned and conducted particle size distribution measurements jointly with Juha Heikkilä. I built and operated the HTDMA system and conducted the data-analysis for particle measurements. I also decided the contents of the paper and, with minor contribution from other authors, wrote the paper.

Paper 4: I had the main responsibility in planning and conducting the oxidation measurements and collecting the TEM samples. I performed the data-analysis of the oxidation measurements. Further, I decided the contents of the paper and I had the main resposibility for writing the paper.

Symbols and abbreviations

BTL	Biomass to liquid
CA	Crank angle
CO	Carbon monoxide
CPC	Condensation particle counter
DMA	Differential mobility analyzer
DME	Dimethyl ether
DNPE	Di-n-pentyl ether
DR	Dilution ratio
EC	Elemental carbon
EELS	Electron energy loss spectrum/spectrometry
EGR	Exhaust gas recirculation
ELNES	Electron energy loss near-edge structure
ELPI	Electrical low-pressure impactor
EN590	Current diesel fuel standard in Europe
FAME	Fatty acid methyl ester
FSN	Filter smoke number
FT	Fisher-Tropsch
GMD	Geometric mean diameter
HC	Hydrocarbons
HR-TEM	High resolution TEM
HTDMA	Hygroscopic TDMA
HTO-TDMA	High temperature oxidation TDMA
HVO	Hydrotreated vegetable oil
IVC	Intake valve closing
N_{tot}	Total particle number (emission)
NO_x	Total of mono-nitrogen oxides (NO and NO_2)
OC	Organic carbon
P_{inj}	Fuel injection pressure
PAH	Polyaromatic hydrocarbon
PM	Particulate matter, i.e. mass of exhaust collected on a filter
RH	Relative humidity
SMPS	Scanning mobility particle sizer
SOI	Start of fuel injection
TDMA	Tandem differential mobility analyzer
TEM	Transmission electron microscope/microscopy
VVA	Variable valve actuator
VVT	Variable valve timing

Contents

Chapter 1

Introduction

"We are not running out of oil, but we are running out of oil that can be produced easily and cheaply" claims a recent comment published in Nature (Murray and King 2012). The grounds for this claim are that it seems we have reached an oil production peak in around 2005. Reaching the peak means that the supply of oil is no longer able to meet the demand leading to oil price swings which, possibly, are one of the reasons behind the current economic crisis (Murray and King 2012). Because of the impact of oil to the economy, and due to the fact that oil reserves on the world are quite localized to certain regions, it is not surprising that alternatives to oil are being researched in different fields of industry. Of these fields, transportation is the highest consumer of oil being responsible for 61.4 % (in 2008) of the annual overall consumption (IEA 2010).

One route to ease the problem in the transportation sector is to add renewable fuel components to the fossil fuel or, further, substitute the fossil fuel with renewable fuel altogether. Using renewable fuel in a combustion engine is not a new idea. Already at the 1900 World's Fair in Paris, a small diesel engine built for petroleum was used with peanut oil although only a few insiders knew about the situation (Knothe et al. 2005). After that, the progress in diesel engine technology has led to the use of less viscous fluids favouring fuels based on crude oil. However, the crises about the supply of mineral oil in 1970s and 1990s have rekindled the interest to use renewable components in fuels (Körbitz 1999).

The use of renewable fuels has also potential to be a part of the solution to ease the current environmental crisis of climate change. Since the start of the industrial era (approximately 1750), human activities have had a warming effect on climate mainly caused by burning fossil fuels (Le Treut et al. 2007). If left unhindered, the climate change can lead to, for example, more intense tropical storms, more frequent heat waves, a rise of the sea level, more frequent heavy precipitation events and an increase in the area affected by droughts (Pachauri and Reisinger 2007). Increasing the share of renewable energy is one path to reduce the net emissions of greenhouse gases and, thus, mitigate the effects of the climate change.

The biofuel that has been used most extensively so far as an addition to as well as a replacement for fossil diesel is biodiesel. Biodiesel can be defined as monoalkyl esters of vegetable oils or animal fats (Demirbas 2007a). Thus, the term fatty acid methyl esters

(FAME) is often used instead of biodiesel. Biodiesels have been produced from variable feedstocks including palm oil (Kalam and Masjuki 2002), jathorpha (Jain and Sharma 2010), soybean (Chang et al. 1996) and rapeseed (Labeckas and Slavinskas 2006) to name a few and they are commercially available. Other promising biofuels for diesel engines are dimethyl ether (DME, Semelsberger et al. (2006)) and paraffinic diesels such as Fischer-Tropsch (FT) diesel (Dry 2002) and hydrotreated vegetable oils (HVO, Rantanen et al. (2005)). From these DME is a gaseous compound in room temperature so it requires new storage and fuel delivery systems (Semelsberger et al. 2006). FT diesel can be produced from coal, natural gas or biomass (Demirbas 2007b). The fuel is paraffinic, it can be blended to conventional diesel at random proportions and no engine modifications are required (Huang et al. 2008). Unfortunately, the production costs of FT-diesel from biomass feedstock have not been competitive enough with conventional diesel prices to enable commercial production (Tijmensen et al. 2002). HVO fuel has very similar composition compared to FT diesel and, thus, it shares its advantages, for example, regarding engine modifications (Kuronen et al. 2007). However, HVO fuel is already being produced commercially.

Besides reducing the dependence of crude oil and potential to reduce greenhouse gas emissions, the mentioned renewable diesels have the advantage to reduce certain exhaust emission components. Using FAME has been shown to noticeably reduce particulate emission mainly due to the oxygen content in the fuel (Lapuerta et al. 2008). For the same reason DME reduces particulate emissions practically to zero (Sorenson 2001). For these fuels NO_x emissions increase somewhat but the increase is small compared to the reduction in particulates (Lapuerta et al. 2008). FT fuels as well as HVO fuels have been shown to reduce all regulated (PM, CO, HC, NO_x) emissions (Gill et al. 2011a; Kuronen et al. 2007; Aatola et al. 2008). Most of this property is associated with the absence of aromatics in FT and HVO fuels. The reasons behind the emission reductions achieved with high cetane number paraffinic diesel fuels are discussed in more detail in Section 3.2 of this thesis.

The reductions in particulate emissions achieved by using the mentioned renewable diesels are welcome as emitted diesel particles have been associated with adverse health effects. Correlations between ambient nanoparticle concentration and mortality has been found on several studies (e.g. Dockery et al. 1993; Laden et al. 2006; Pope III et al. 2009) but the exact mechanisms by which the particles affect health are still largely unknown and currently under intensive research. So far diesel particles have been associated with cardiovascular diseases (Miller et al. 2007; Mills et al. 2008) and sufficiently small particles have been shown to be able to enter the bloodstream through lungs and even reach the brain (Oberdörster et al. 2004). In June 2012, World Health Organization even promoted the classification of diesel exhaust from *probably carcinogenic to humans* (Group 2A) to *carsinogenic to humans* (Group 1)

based on *sufficient evidence* (WHO 2012). Globally, but especially in Europe and in the USA, the increased knowledge of adverse health effects of diesel particles has led to stricter regularization of particulate emissions. Due to the particle reducing potential of renewable diesel fuels, they can be a part of the solution to reach the emission limits together with exhaust aftertreatment techniques and engine optimization.

Not only the amount of emitted particles but also the properties of the particles may alter as a consequence of changing the fuel from fossil diesel to renewable diesel (e.g. Jung et al. 2006; Lapuerta et al. 2012). These properties include, for example, the amount of semivolatile matter on the particles (volatility), the eagerness of particles to oxidize (oxidizability/reactivity) and the ability of particles to take on water (hygroscopicity). These properties are important since they provide information on the behaviour of emitted particles in aftertreatment devices, in the atmosphere and, further, in human respiratory system.

As it has been already shown that HVO fuel reduces several exhaust emissions, this thesis will take the research to a step further. This thesis aims to show how exhaust emissions from a HVO-fueled engine can be further reduced and how the use of HVO-based fuel affects exhaust particle properties. The applied methods to reduce exhaust emissions studied in this thesis are engine optimization via variable valve timing (**Paper 1**), multiparameter engine optimization (injection timing, valve timing, exhaust gas recirculation, injection pressure, **Paper 2**) and an addition of oxygenate to the HVO fuel (**Paper 3**). The chosen methods are, of course, only a fraction of possible techniques to control exhaust emissions of a diesel engine but, according to the author's knowledge, they have not been previously applied to renewable fuels. Thus, this thesis studies some new paths for emissions reductions with renewable diesel. The emissions considered in this thesis are primarily particulate and NO_x emissions since these two emission components are the main targets of the upcoming Euro VI emission legislation in Europe.

In **Paper 3** and **Paper 4**, the effects of different fuels on exhaust particles have been studied by using tandem differential mobility analyzer (TDMA) techniques. These techniques enabled the studying of hygroscopic and oxidation properties of emitted particles. The development of the required measurement equipment with the aim of using them at measurement sites was also a significant part of this thesis.

Chapter 2

Diesel engine exhaust emissions: an overview

2.1 Exhaust emissions and regulations

The main emissions of diesel exhaust are CO, oxides of nitrogen (NO and NO_2, collectively known as NO_x), unburned or partly burned volatile hydrocarbons (HC) and soot particles. From the mentioned emissions, soot, CO and HC are formed due to incomplete combustion. However, when these emissions are reduced by increasing combustion temperature, NO_x emissions are generally increased. This is caused by the chemical reactions involving oxygen and nitrogen in a high temperature environment. The high temperature shifts the chemical equilibrium to become favourable for rapid NO_x formation but the subsequent cooling of the exhaust gas traps the gases in their high temperature equilibrium concentrations (Fernando et al. 2006). There can also be oxides of sulphur in the exhaust. Sulphur comes to the combustion process from the fuel and the lubricant. During combustion, sulphur is mainly oxidized to SO_2, but a small amount can be oxidized to sulphur trioxide (SO_3), which combines with water to form sulphuric acid. The suphuric acid then either condensates on existing soot particles or form new particles via nucleation.

In Europe, on-road engine exhaust emissions have been regulated since 1992, and the regulations have become stricter ever since (Dieselnet 2012). Table 2.1 presents the current and the future emission limits for heavy-duty diesel engines in Europe. As

Table 2.1: The latest exhaust emission limits (g/kWh) for heavy-duty diesel engines over ESC cycle according to European regulations (Dieselnet 2012)

Tier	CO	HC	NO_x	PM
Euro V (2008)	1.5	0.46	2.0	0.02
Euro VI (2013)	1.5	0.13	0.4	0.01

it can be seen, the most radical reduction, 80 % compared to Euro V limit, in the future Euro VI standard is going to be in NO_x emissions. Moreover, at the same time the allowed particulate matter (PM) emission will be halved. Therefore, overcoming the trade-off between PM and NO_x thus enabling the simultaneous decrease in both of these emissions is perhaps the most challenging problem in meeting the future Euro VI standard. In addition to the particle mass limit, also a particle number limit ($8{\cdot}10^{11}$ #/kWh over the WHSC cycle with a measurement system based on the work of the Particulate Measurement Programme (PMP), EU (2011)) will be introduced to emission regulations. The particle number limit has been introduced to ensure that emission regulations are not met with technology that produces large amounts of small nanoparticles.

2.2 Exhaust particles

The formation of exhaust particles begins by the formation of soot in the high temperature, fuel-rich reaction zone around individual fuel droplets (Neeft et al. 1996). First, molecular precursors of soot, namely acetylene and heavy PAHs, are formed by pyrolysis and/or oxidation of fuel molecules (Heywood 1988; Xi and Zhong 2006). The precursor soot then grows in size via nucleation/inception, surface growth, condensation and coagulation (Neeft et al. 1996; Xi and Zhong 2006). The resulting "primary" soot particles, which are still near spherical, then leave the cylinder and coagulate further to form agglomerates (Neeft et al. 1996). Furthermore, oxidation is present in all stages of soot formation and it occurs on the surface of soot particles. There is considerable agreement on these general features of soot particle formation but many underlying mechanisms especially relating to nucleation and surface growth are still relatively poorly understood (Xi and Zhong 2006).

When the exhaust gas cools down in the exhaust pipe and during dilution, hydrocarbons of relatively low volatility, sulphates and sulphuric acid adsorb and condense on the soot (Neeft et al. 1996). In addition to adsorption and condensation, these compounds can also be transformed to solid and liquid particulate matter via nucleation, i.e. the formation of new nanoparticles (Kittelson 1998). However, some recent studies indicate that there might be also non-volatile particles in the size range of these so called nucleation particles or small non-volatile cores within some of the particles that have been generally assumed to be volatile (Rönkkö et al. 2007; Lähde et al. 2008; Filippo and Maricq 2008). An overall schematic of the composition and structure of diesel exhaust nanoparticles is shown in Figure 2.1.

When exhaust particles are sorted by size, generally three separate particle modes can be observed (Kittelson 1998). These modes are usually quite near lognormal in shape and they are termed as nucleation, accumulation and coarse modes. The

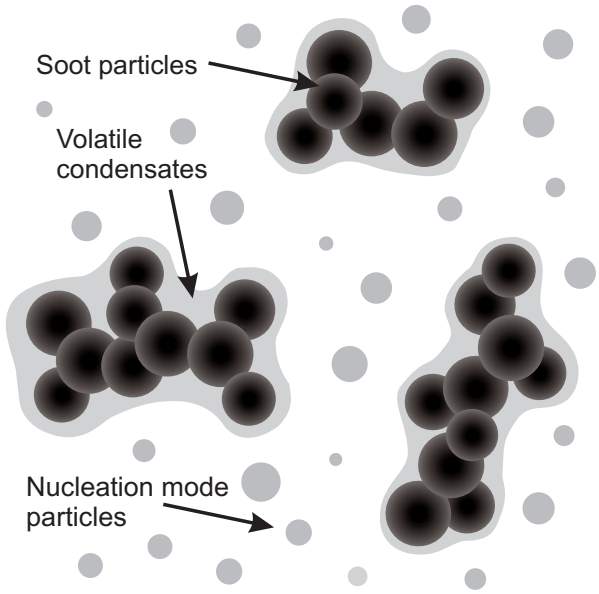

Figure 2.1: A schematic of the composition and structure of diesel exhaust nanoparticles.

nucleation mode is typically 5–50 nm in size and it consists of the mentioned nucleation particles. It may contribute over 90 % of the total particle number (Kittelson 1998) although its mass content is often low. The nucleation mode has also been observed to be quite sensitive to the dilution of the exhaust (Eastwood 2008). Most of the total particulate mass exists in the accumulation mode. Accumulation particles are generally under 300 nm in diameter and they consists of soot agglomerates coated by adsorbed material (Kittelson 1998). The coarse mode consists of accumulation mode particles that have deposited in the exhaust system and later re-entered the exhaust stream as much larger particles, over 1 μm in diameter (Eastwood 2008). This storage-release makes the coarse mode particle emission inconsistent which is one of the reasons why this thesis will concentrate on particles belonging to the other two modes.

2.3 Measuring emissions

Particle sampling may cause unintentional transformations in the sampled aerosol. Depending on sampling and dilution conditions, the degree of condensation and nucleation of volatile hydrocarbons, particle losses and the amount of coagulation occurring before the measurement instruments may vary. In this thesis, two different sampling/dilution systems were applied. These systems will be now described shortly.

The sampling and dilution system applied in **Paper 1**, **Paper 2** and **Paper 3** was based on a system developed for the "Particulates" research program of the EU (Ntziachristos et al. 2004). The sampled particles were first diluted by a porous tube diluter (Mikkanen et al. 2001) which had low particle losses and allowed nucleation of volatile compounds. A dilution ratio of 12 was used in the porous tube diluter as there is evidence that the chosen dilution ratio allows the imitation of nucleation particle formation in real world (Rönkkö et al. 2006). A dilution air temperature of 30 °C was used in line with the "Particulates" system. The porous tube diluter was followed by an aging chamber (volume 2.3 dm^3) to allow the possibly formed nucleation mode to grow to measurable particle sizes (Vaaraslahti et al. 2004). The sample was then further diluted with an ejector diluter in order to reduce the particle concentrations to the range of the measurement instruments. According to Giechaskiel et al. (2009), the ejector diluter does not change the characteristics of particle size distribution so it can be safely used to further dilute the already diluted exhaust. The dilution ratio of the system was obtained by comparing the raw and diluted CO_2 concentrations.

A thermodenuder was also applied either to study the volatility of exhaust particles (**Paper 1**, **Paper 2**) or to ensure that the sampled particles were free of volatile compounds (**Paper 4**). The principle of the thermodenuder treatment is to first heat the aerosol sample to a high enough temperature (in this thesis 265 °C), so that the possibly condensated volatile compounds on the exhaust particles evaporate, and then to absorb the evaporated compounds to a layer of active charcoal in order to avoid recondensation/nucleation. The flow rate through the thermodenuder was typically approximately 12 lpm. A schematic of the measurement setup applied in **Paper 1**, **Paper 2** and **Paper 3** is presented in Figure 2.2.

In **Paper 1**, **Paper 2** and **Paper 3**, particle number and particle size distribution measurements were conducted with condensation particle counters (CPC, Cheng (2011)) and scanning mobility particle sizers (SMPS, Wang and Flagan (1990)), respectively. In addition, an electrical low pressure impactor (ELPI, Keskinen et al. (1992)) was always used together with the mentioned instruments to ensure that the exhaust sample was stable during the measurements.

Particulate matter (PM) mass measurements were conducted using a separate sampling line with an AVL SPC 472 micro dilution tunnel according to the ISO 8178-1:2006 standard whereas NO_x measurements were measured with an Eco Physics CLD 822 S h analyzer through a heated sample line.

The discussed measurement instruments primarily measure emission concentrations. Nevertheless, concentration is not the optimal quantity in representing exhaust emissions since it does not take into account the differences in the exhaust mass flows in different engine conditions. Therefore, the emissions of PM, N_{tot} and NO_x presented in this thesis are converted to the units of [emission]/kWh. This is performed by using the

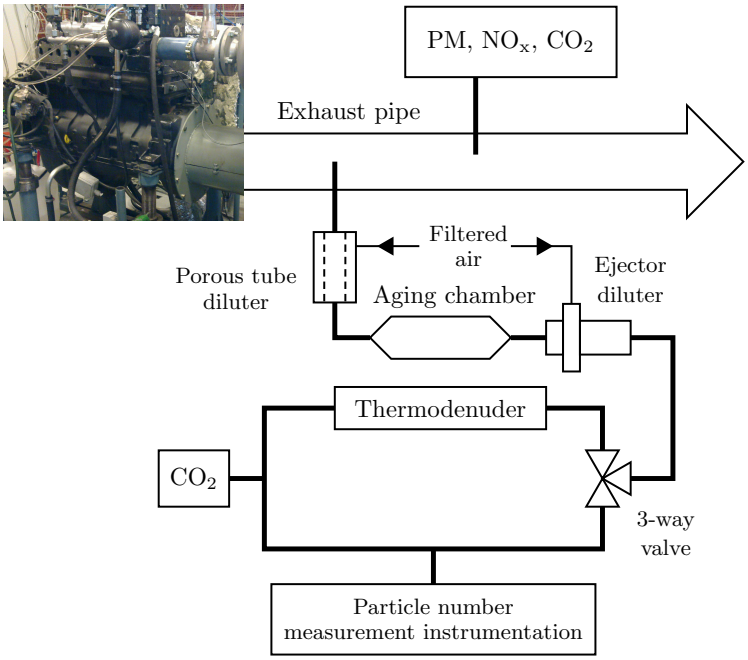

Figure 2.2: Measurement setup applied in **Paper 1**, **Paper 2** and **Paper 3**. Figure modified from **Paper 1**.

following equation:

$$\frac{X}{E} = x\frac{\dot{m}_{\text{exh}}}{\rho_{\text{air}} P_{\text{ind}}}, \tag{2.1}$$

where X is the absolute emission in question, x is the emission concentration in question (e.g. in units $\#/\text{cm}^3$), E is energy (kWh), $\dot{m}_{\text{exh}}$ is the exhaust mass flow, ρ_{air} is the density of exhaust air at the measurement temperature and P_{ind} is the indicated power of the engine.

In **Paper 4**, the dilution was performed by a heated ejector diluter. The heated ejector pump sampling has been applied previously by e.g. Maricq et al. (1999) and Lyyränen et al. (2004). Heating of the primary ejector diluter is required to avoid the blocking of the ejector nozzle due to thermophoretic and vapour deposition (Lyyränen et al. 2004). Due to the small temperature difference between the primary dilution air and exhaust gas, the condensation and nucleation of volatile compounds can be mostly avoided. Normally the heated ejector diluter is followed by a cold ejector as a secondary diluter. However, as the focus in **Paper 4** was not on the concentration but on the properties of soot particles, and as a high concentration of particles was required, only the primary ejector diluter was used. A more detailed description of the

measurement system of **Paper 4** is presented later in Chapter 5.

Chapter 3

Hydrotreated vegetable oil diesel fuel

3.1 Chemical composition and production

Hydrotreated vegetable oil (HVO) is renewable diesel fuel that can be blended to fossil diesel or used as such (Kuronen et al. 2007). Hydrotreated vegetable oil (HVO) fuel composes of long chain n- and iso-paraffins (C_nH_{2n+2}) (Rantanen et al. 2005). As fully paraffinic fuel, HVO contains practically no sulphur, oxygen or aromatics. Typical HVO fuel properties and, for comparison, typical diesel fuel properties are presented in Table 3.1. The compared typical diesel fuel met the European EN590 diesel fuel standard. The most dramatic differences between fossil EN590 diesel fuel and HVO fuel are cetane number and density. In fact, the low density value of HVO is the reason why HVO does not meet the EN590 specification in which the lower density limit is 820 kg/m^3 (Dieselnet 2012). However, up to 30 % HVO can be blended into fossil diesel while still meeting the specification. Cetane number describes fuel ignition quality. More specifically, cetane number is a measure of the ignition delay of the fuel (Heywood 1988). The higher is cetane number the shorter is the ignition delay. Pure HVO, in general, has very low lubricity due to the absence of sulphur and oxygen compounds (Lapuerta et al. 2011). However, similar doses of additives that are used to improve the lubricity of ultra-low sulphur diesels (ULSD) can be used to improve the lubricity of HVO fuel also (Kuronen et al. 2007).

Due to the lower volumetric heating value of HVO, a larger volume of HVO is required in order to achieve a given load point. Thus, the volumetric fuel consumption increases compared to EN590 diesel fuel. However, as the density of HVO is lower than that of EN590 diesel, the mass based fuel consumption actually decreases with HVO.

HVO is produced by hydrogenating the double bonds and removing the oxygen from the triglyceride chain of the vegetable oil (Lapuerta et al. 2011). In addition to the feedstock oil, the process requires hydrogen and produces n- and iso-alkanes as end products. Propane, water and CO or CO_2 are produced as byproducts. A more detailed account of the chemical process is described, for example, by Huber and Corma (2007), Helwani et al. (2009) and Lapuerta et al. (2011). Fatty acids from

Table 3.1: Typical fuel properties of HVO fuel and European EN590 summer grade diesel fuel (Kuronen et al. 2007). The HVO fuel includes lubricity additive.

	HVO	EN590
density at 15 °C (kg/m^3)	775–785	835
viscosity 40 °C (mm^2/s)	2.9–3.5	3.5
distillation area (°C)	190–320	180–360
cloud point (°C)	(−25)–(−5)	−5
lower heating value (MJ/kg)	44	42.7
lower heating value (MJ/l)	34.4	35.7
cetane number	80–99	53
total aromatics (wt-%)	0	30
oxygen content (wt-%)	0	0
sulfur content (mg/kg)	<10	<10
HFRR lubricity at 60 °C (μm)	<460	<460

vegetable oils or animal fats can be used as feedstock to produce HVO (Rantanen et al. 2005). Companies that advertise renewable diesel fuels by hydrotreating vegetable oils include Universal Oil Products (UOP), Syntroleum, Petrobras, ConocoPhillips and Neste Oil (Lapuerta et al. 2011).

To provide better understanding of HVO fuel compared to other renewable diesels, it is also worth to shortly describe the production processes of two other technologies applicable for producing renewable diesel. The first and most common technology for producing diesel fuel from renewable feedstock is subjecting vegetable oils or animal fats to a transesterification reaction (Knothe et al. 2005). In transesterification, the vegetable oil or animal fat is reacted with an alcohol (usually methanol) in the presence of a catalyst. The reaction produces corresponding alkyl esters of feedstock oils and fats. If methanol is used as the alcohol, the final product is fatty acid methyl esters (FAME) which can be used as diesel fuel. The term *biodiesel* is often used exclusively for fuels produced via transesterification.

Another method to produce renewable fuel from biomass feedstock is via Fischer-Tropsch (FT) synthesis. The synthesis produces synthetic olefins and/or paraffins of different lengths from syngas, i.e. a gas mixture of H_2 and CO (Demirbas 2007b; Gill et al. 2011a). The required syngas can be produced from natural gas, coal or biomass feedstock (Gill et al. 2011a). From coal or biomass, the syngas can be produced by steam gasification processes (Demirbas 2007b). The large hydrocarbons produced by the FT synthesis can then be hydrocracked and any formed oxygenates can be removed

during post-processing. The end product is high quality diesel fuel that has high cetane number and is virtually free from aromatics or suphur (Gill et al. 2011a).

Thus, HVO fuel is chemically very similar to fuels produced using FT synthesis (Aatola et al. 2008). Paraffinic renewable fuels in general are more readily accepted by engine manufacturers and fuel distributors than transesterified biodiesels as paraffinic fuels have better storage stability (Kuronen et al. 2007). This enables the distribution of HVO and FT diesels with the current fuel logistics. It has been also reported that in most cases HVO outperforms transesterified biodiesels regarding the lifecycle environmental impacts of the fuels when produced from the same feedstock (Sunde et al. 2011).

The HVO fuel that has been used in this thesis is produced by Neste Oil (Rantanen et al. 2005) and branded as NExBTL. The fuel is produced using mainly palm oil as feedstock.

3.2 Exhaust emissions

Prior to the work in this thesis, quite few articles had studied the exhaust emission of a diesel engine run using HVO as fuel. Rantanen et al. (2005) studied the emissions with maximum of 85 vol-% HVO blended to fossil diesel using three light duty cars and concluded that hydrocarbon (HC) and carbon monoxide (CO) concentration as well as particulate matter (PM) emission decreased with HVO blends but no clear decrease in NO_x emission was observed. Kuronen et al. (2007) and Murtonen et al. (2010) studied emissions with heavy-duty engines, mainly buses, using neat HVO fuel. Some of the studied engines used aftertreatment devices and some used exhaust gas recirculation (EGR). Reported decreases were 3–28 % in NO_x emission and 17–51 % in PM when the fuel was changed from fossil EN590 fuel to HVO. Decreases were observed also in CO and HC emissions as well as in aldehyde and polyaromatic hydrocarbon (PAH) emissions (Murtonen et al. 2010). Also Aatola et al. (2008) compared the emissions with fossil EN590 fuel with neat HVO with a heavy-duty engine and obtained 35 % decrease in smoke and 5 % decrease in NO_x with HVO on average.

In **Paper 1**, particulate and NO_x emissions of a single cylinder research engine, which was used also in **Paper 2** and **Paper 3**, were studied both with fossil EN590 fuel as well as with HVO. The engine used manufacturer's engine settings for each load condition, and there were no aftertreatment devices installed to the engine. PM and NO_x emissions of the engine with three different engine loads (50, 75 and 100 %) are shown in Figure 3.1. The decrease in PM emission with HVO was roughly 30–40 % depending on load (the 40 % decrease was observed at the highest load) compared to EN590 fuel. In addition, HVO decreased also NO_x emissions roughly 3–6 % (lowest decrease with 100 % load). Thus, the decrease in PM and in NO_x with the engine was

in line with the mentioned previous studies.

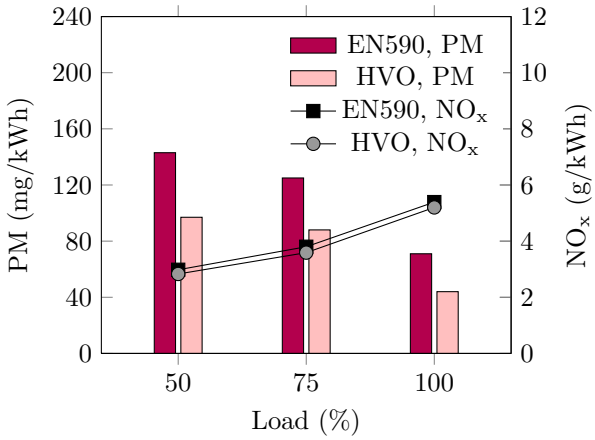

Figure 3.1: Particulate mass (PM) and NO_x emissions with HVO fuel and fossil EN590 fuel. The measurements were performed using a single-cylinder research engine. Modified from **Paper 1**.

The main reasons for the lower PM emission with HVO fuel are probably the lower aromatic hydrocarbon concentration and the higher cetane number of HVO fuel. Most studies have shown that higher aromatic concentrations in fuel lead to higher particulate emissions although, in some cases, the effect of aromatics is disguised by, for example, the engine model and calibration (Eastwood 2008). Cetane number, on the other hand, affects the ignition delay of the fuel. In the case of the research engine of **Paper 1**, the manufacturer's setting for the fuel injection was quite late in order to reduce NO_x formation. Thus, as the higher cetane number advanced the ignition, the combustion phasing became more optimal for fuel combustion and the soot formation was somewhat suppressed. In some cases, the higher cetane number and, thus, shorter ignition delay may lead to increased particulate emission due to lower initial burning and long combustion duration (Kidoguchi et al. 2000). In general, there are studies reporting both positive and negative correlations between cetane number and particulate emissions (Eastwood 2008). The main problem with studying the effects of cetane number (and aromaticity) is that they are easily mixed to the effects of other fuel and engine parameters. Armas et al. (2010) attacked this problem by matching the combustion phasing and obtaining a similar rate of heat release between the tested fuels (ultra low sulphur diesel, FT diesel and FAME) by adjusting fuel injection timing and fuel rail pressure. They reported that with matched phasing, FT fuel reduced both PM and NO_x emissions but the reduction was lower than in the original, non-matched case. Also the fact that using the HVO instead of fossil EN590

increases the indicated efficiency of the engine (see **Paper 1**) will surely reduce the emission somewhat. The reason to this is that with higher efficiency the same load can be achieved with reduced mass of fuel. This increases the relative air to fuel ratio which, further, promotes the combustion (Huang et al. 2008).

One of the reasons for higher NO_x emissions for EN590 diesel fuel compared to HVO fuel could be that aromatic compounds have higher adiabatic flame temperature and a lower H/C-ratio. As aromatic compounds produce higher local combustion temperatures (Glaude et al. 2010), NO_x formation is promoted with fuels having higher aromatic content. Aatola et al. (2008), on the other hand, suggested that the shorter ignition delay and lower volumetric heating value of HVO could increase the combustion time of the fuel resulting to lower temperature and, thereby, to lower NO_x emission. The higher cetane number and, thus, the shorter ignition delay of HVO also reduces the energy released in the premixed combustion phase which reduces the maximum combustion temperature and pressure in the cylinder leading to suppressed NO_x formation (Huang et al. 2008).

Particle size distributions measured with HVO and with fossil EN590 fuel are presented in Figure 3.2. The total particle number emission in the figure was obtained from the distribution. Depending on load, the total particle number emission decreased 13–27 % with HVO fuel. The largest decrease (6.5 nm, 10 %) in GMD was observed with 50 % load conditions. The decrease in GMD was probably due to the reduced exhaust particle number concentration which suppressed particle growth by coagulation. The volatility of the exhaust particles was low enough that no change in geometric mean diameter (GMD) was observed with thermodenuder treatment. This is in line with the low gaseous HC emission (less than 0.1 g/kWh at most) with both fuels. Overall, the HVO fuel produced quite similar exhaust particle size distributions than EN590. Both produced unimodal distributions with GMDs in the range of 62–67 nm. The particle number emission results are in agreement with those presented in the previous HVO studies (Rantanen et al. 2005; Kuronen et al. 2007; Murtonen et al. 2010).

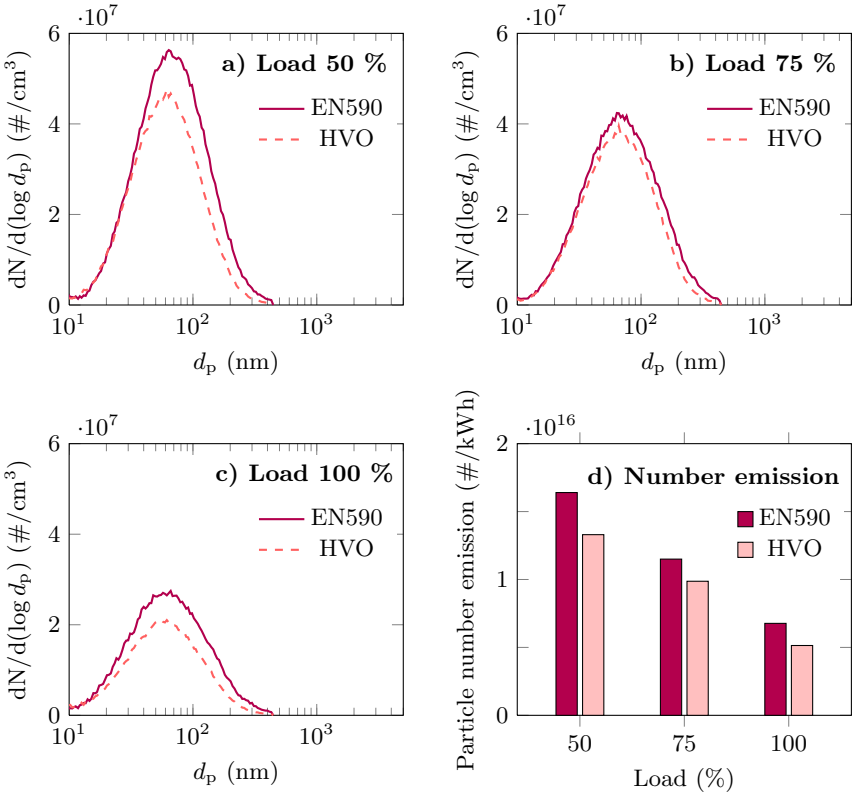

Figure 3.2: Particle number distributions of a research engine with 50 (a), 75 (b) and 100 % (c) loads with both HVO fuel and fossil EN590 fuel. Also total number concentrations emitted with different fuels and loads are presented (d). Modified from **Paper 1**.

Chapter 4

Techniques to reduce emissions

4.1 Engine parameter adjustments

To abate diesel exhaust emissions, one either has to influence on the combustion process or to prevent somehow the formed emissions from reaching the atmosphere. The former approach of emission abatement can be realized by influencing on the fuel and the lubricant or by adjusting the engine. Possible engine adjustments include e.g. optimizing the injector nozzle or the geometry of the combustion chamber, adjusting injection pressure, intake air pressure, injection timing and valve timings or applying exhaust gas recirculation (EGR). For the latter approach, different aftertreatment devices such as particulate filters, oxidations catalysts and deNO_x-catalysts can be used. In this thesis, the emission reduction techniques for the HVO fuel are limited to influencing the fuel, which is presented in the next section, and to adjusting engine parameters (injection timing, valve timing, EGR and injection pressure), which is discussed here.

As HVO fuel differs from the common diesel fuel, e.g. in respects of cetane number and density, the original engine adjustments set by the manufacturer and chosen for common diesel fuel might not be optimal for HVO fuel. Aatola et al. (2008) concluded in their study that optimization of injection parameters for HVO allows more significant reductions in exhaust emissions compared to EN590 diesel fuel than those obtainable by only changing the EN590 to HVO fuel.

The possibility to further diminish exhaust emissions with engine optimization has not escaped attention in the case of other alternative fuels either. For example, optimization of injection timing, injection pressure and EGR percentage have been studied with biodiesel (Leung et al. 2006; Bunce et al. 2011) and optimization of injection timing with FT diesel fuels (Abu-Jrai et al. 2006; Wu et al. 2007). However, a less explored area in the field of alternative diesel fuels is the application of variable valve timing (VVT). In VVT, the timing, duration and lift of the intake and/or exhaust valve is altered during engine operation. VVT has been mostly associated with spark ignition engines and, in this context, Hong et al. (2004) present a quite thorough review

of different VVT strategies. The use of the strategies becomes more limited when VVT is applied to a modern diesel engine due to the very small clearance between the piston and valves in the engine (Lancefield et al. 2000). In diesel engines, the main aim in utilizing VVT is to achieve reductions in exhaust emissions (Benajes et al. 2008).

Here, the VVT strategy considered is the advance of intake valve closure (IVC). Advanced IVC reduces the effective compression ratio and, without an increase in intake air pressure, also the air/fuel ratio in the cylinder (Benajes et al. 2009a). These changes reduce peak temperature and pressure in the cylinder and increase the auto-ignition delay time of the fuel. The reduction of combustion temperature reduces NO_x formation but, due to the reduction in the air/fuel ratio and cylinder temperature, particle emissions are increased. Advanced IVC, without alterations in intake air pressure, has been studied by e.g. Wang et al. (2005), Benajes et al. (2009a) and Benajes et al. (2009b). Benajes et al. (2009b) named this sort of cycle as a modern version of Atkinson cycle. Reason to this is that advanced (or retarded) IVC shortens the effective intake and compression strokes compared to the corresponding expansion stroke. In the original Atkinson cycle, the expansion stroke would continue as far as to the exhaust pressure (Heywood 1988).

Benajes et al. (2009a) suggest that the most critical drawbacks of early IVC, for example the sharp increase in soot emissions, should be diminished if, while advancing IVC, the intake pressure is boosted accordingly. Thus, the reduction in the amount of intake air mass could be avoided and the nominal air/fuel ratio could be maintained. The resulting engine cycle will be referred from now on as the Miller cycle (Benajes et al. 2009b; Miller 1947). The use of the Miller cycle does not significantly alter the nominal density or pressure at the top dead center of the cylinder but the reduction in peak temperature, and thus in NO_x, should be comparable to the modern Atkinson cycle discussed earlier (Benajes et al. 2009a). Benajes et al. (2008) studied the Miller cycle using retarded IVC strategy together with different injection timings. They observed that the ignition delay and fuel consumption increased somewhat with the Miller cycle but both soot and NO_x emissions were decreased.

The suitability of the Miller cycle via advanced IVC for HVO was studied in **Paper 1**. The engine used in the study was a single cylinder research engine based on a commercial 6-cylinder off-road common rail diesel engine. The studied advances of IVC were 0, 30, 50 and 70 °CA (crank angle degrees) before the standard IVC angle set by the engine manufacturer. To achieve the Miller cycle, the intake air pressure was increased accordingly in order to avoid reductions in the intake air mass. In addition to IVC, fuel injection timing was also altered in order to study the combined effect of early IVC and adjusted injection timing. Particle number (N_{tot}) and NO_x emissions of the study are presented in Figure 4.1. These tests were performed on the 100 % load.

As it can be seen from the figure, advancing IVC to realize the Miller cycle decreased

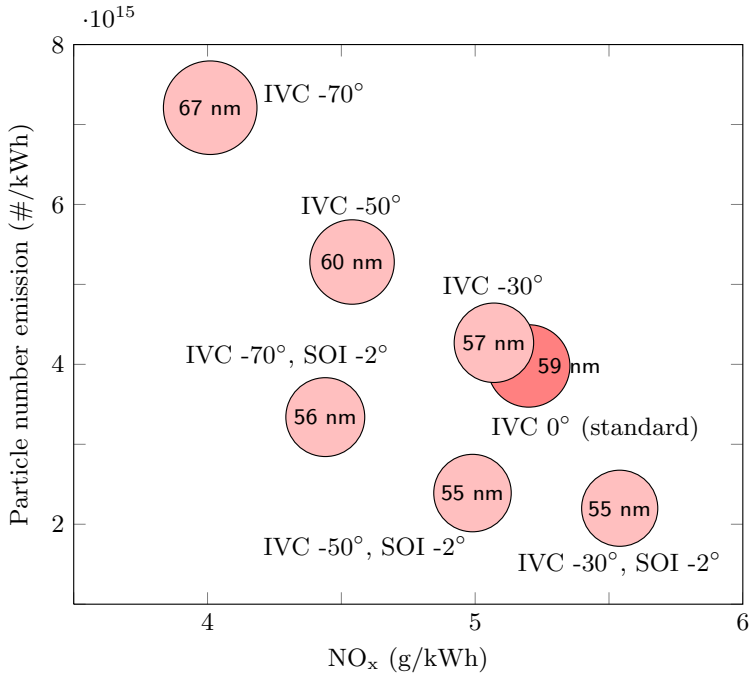

Figure 4.1: Particle number and NO_x emission, as well as the GMDs of the measured particle size distributions, with different IVC and SOI timings on the 100 % load. Modified from **Paper 1**.

NO_x emission but increased N_{tot} as well as the particle size. Similar results have been reported by Imperato et al. (2010) although they used filter smoke number (FSN) as a measure of particulates. The initial 30 °CA advance of IVC resulted in quite small changes in the emissions but, as the IVC advance was increased, the increase in N_{tot} and the decrease in NO_x became more pronounced. As presented in Table 1 of **Paper 1**, specific fuel consumption (g/kWh) remained quite unchanged as a result of advancing IVC.

Since advancing IVC reduces NO_x formation due to the lower peak temperature of the cylinder, this provides an opportunity to reduce also soot particle formation by allowing better combustion conditions. One method to realize better combustion is to shift the start of fuel ignition towards the top dead center via adjustments in injection timing. The advance of 2 °CA in the start of injection (SOI) in combination with the studied IVC timings is also presented in Figure 4.1. The figure shows that advancing SOI together with advanced IVC allows a simultaneous decrease in both N_{tot} and NO_x. However, it should be noted that the SOI of the studied engine was originally set quite late (see Table 4.1) in order to limit NO_x emissions.

In order to study further how much the optimization of an engine run with HVO fuel could reduce exhaust emissions without significant drawbacks in the performance of the engine, more diverse adjustments of engine parameters were performed using the same engine as in **Paper 1**. In **Paper 2**, simultaneus adjustments of injection timing, injection pressure, intake valve timing and EGR percentage was applied in order to better utilize the benefits of the HVO fuel. In fact, **Paper 2** presents the first HVO study where more than two engine parameteres have been simultaneusly balanced in order to optimize the engine.

Three target conditions were chosen for the adjustments. These were low-NO_x (LN) and low-smoke (LS) conditions and a condition where both NO_x and particle emissions were relatively low (LNLS). The adjustments were performed on the 50, 75 and 100 % engine loads by using advanced IVC and adjusted SOI, EGR and fuel injection pressure (P_{inj}). EGR was simulated by supplying neat nitrogen gas in the charge air. The studied engine conditions are shown in Table 4.1. The indicated mean effective pressures of the 50, 75 and 100 % loads were 10.8, 16.2 and 21.4 bar, respectively. The standard settings mentioned in the table refer to the engine settings provided by the engine manufacturer for each load. The LN and LS conditions represented the cases where one emission, particles or NO_x, can be reduced to the minimum using engine parameter adjustments while the other could be reduced using a suitable aftertreatment device. The LNLS condition, on the other hand, shows how large emission reductions in both particles and NO_x are possible with engine parameter adjustments only.

The Miller cylce with 70 °CA advanced IVC was used in all the studied adjusted conditions. NO_x emissions were further reduced by applying varying percentages of EGR. EGR decreases the oxygen concentration in the cylinder and, thus, increases ignition delay (Ickes et al. 2009). This shifts combustion to later phasing and, thereby, decreases the cylinder peak temperature and pressure. This in turn reduces NO_x formation. Unfortunately, the reductions in oxygen concentration and cylinder temperature hinder the rapid premix-combustion phase and, due to the lower oxygen concentration, the diffusion combustion is also suppressed (Satoh et al. 1997). Consequently, particle emissions are increased.

The increased particle emissions caused by advanced IVC and increased EGR are compensated by increasing fuel injection pressure. Higher fuel injection pressure causes the combustion phasing to advance as the fuel spray breaks up faster and, thus, the mixing time is reduced (Ickes et al. 2009). The advanced phasing enhance the premix-combustion phase which shortens the overall combustion process (Heywood 1988). Due to the better air mixing and higher flame temperatures induced by the enhanced premixed combustion, particle emissions are reduced and NO_x emissions increased (Lähde et al. 2011). At three conditions, the combination of EGR, advanced IVC and higher P_{inj} were also modified by adjusting the SOI timing. At the 50 % LS

Table 4.1: Engine load, power, efficiency (Eff.), IVC, SOI, EGR and P_{inj} of the measured engine conditions. IVC values are relative to the bottom dead center (BDC). Positive values mean after BDC and negative before BDC. The SOI values are relative to the top dead center (TDC). The engine speed was 1500 rpm at all measured conditions. (**Paper 2**)

Load (%)		Power (kW)	Eff. (%)	IVC (deg)	SOI (deg)	EGR (%)	P_{inj} (bar)
50	stand.	18.7	35.7	22	−1.2	0	464
	LN	18.5	39.5	−48	−1.2	10	600
	LS	18.4	41.5	−48	−4.2	2.5	600
	LNLS	18.5	39.6	−48	−1.2	5	600
75	stand.	27.7	37.5	22	−2.1	0	594
	LN	27.7	37.4	−48	−0.1	10	1000
	LS	27.5	40.5	−48	−2.1	2.5	800
	LNLS	27.7	41.8	−48	−2.1	10	1000
100	stand.	36.6	37.3	22	−1.6	0	878
	LN	36.4	41.1	−48	−0.6	12	1400
	LS	36.1	41.1	−48	−1.6	2.5	1200
	LNLS	36.1	41.9	−48	−1.6	10	1400

conditions, SOI was advanced to improve combustion conditions and, at the 75 % and 100 % LN conditions, SOI was retarded to achieve further reductions in NO_x emissions.

Relative changes in particle and NO_x emissions as a result of different adjusted conditions are presented in Figure 4.2. The figure presents the changes relative to the standard engine conditions with HVO fuel. The absolute values of engine emissions are presented in Table 4.2. Applying adjusted conditions did not impose changes in the shape of the particle size distribution.

As it can be seen from Figure 4.2, approximately a 60 % decrease in the NO_x emission was achieved on all the studied loads at LN conditions. As expected, the particle emission simultaneously increased. However, on other than 50 % loads, the PM emission remained under the reference level, i.e. the emission level of the engine run at standard engine settings with EN590 fuel. On the 50 % load, the reference level of PM was exceeded by 17 %. This implies that the 60 % decrease in NO_x emissions might not be achievable on the 50 % load with the studied engine without exceeding the reference level of particle emissions. Relative increase in N_{tot} was on all the studied loads higher than the increase in PM. On the 50 % load, the difference between the changes in N_{tot} and PM was somewhat smaller due to the increase in the geometric

Table 4.2: Total particulate mass (PM), total particle emission (N_{tot}), geometric mean diameter of the particle size distribution (GMD) and nitrogen oxide emissions (NO_x) on the 50, 75 and 100 % loads at standard engine conditions. Modified from **Paper 2**.

Load (%)	PM (mg/kWh)	$N_{tot} \cdot 10^{15}$ (#/kWh)	GMD (nm)	NO_x (g/kWh)
50	99	1.08	61.5	2.97
75	85	0.86	65.5	3.62
100	42	0.42	61.5	5.21

mean diameter of the particle size distribution. On the LN conditions at other loads, a decrease in GMD was observed compared to the standard engine settings.

At the LS conditions, NO_x emission remained at or slightly under the emission at standard engine conditions with HVO. PM emission, on the other hand, was decreased 45–68 % depending on load. On all the studied loads at the LS conditions, GMDs of the particle size distributions were reduced roughly 20 %. By applying the LNLS adjustments, particle number emission remained quite unchanged but GMD, and thus also PM, was decreased. A reduction of 25–33 % was observed in PM at LNLS conditions depending on load together with a 30–50 % decrease in NO_x emission.

As shown in Figure 3.1, mere changing the fuel from EN590 decreases PM emissions 30–40 % depending on load. The results in Figure 4.2 show that the achieved PM emission level could be further reduced over 45 % by adjusting engine parameters with the studied engine without increasing NO_x emissions. Alternatively, NO_x emissions, or both particle and NO_x emissions, could be reduced by engine parameter adjustments.

In Figure 4.3, the LN, LS and LNLS conditions on the 100 % load are compared to the IVC -70 °CA conditions of **Paper 1**. The Figure 4.3 is presented in the same fashion as Figure 4.1 but, in Figure 4.3, PM emission is used instead of particle number emission. The reason to this is that particle number emission was measured with a different particle counter in **Paper 1** (a water based CPC 3786) than in **Paper 2** (a butanol based CPC 3775 in the cloud counting mode) which further led to a difference in the absolute values of the particle number emissions. Nonetheless, the Figure 4.3 illustrates that just by adjusting both IVC and injection timing it is possible to reduce both NO_x and particulate emissions of an HVO-fueled engine. However, the figure also shows that much more pronounced emission reductions can be achieved when the advanced IVC (using constant intake air mass flow) is combined with EGR, higher injection pressure and adjusted injection timing.

It should, nevertheless, be stressed that the emission reduction results obtained

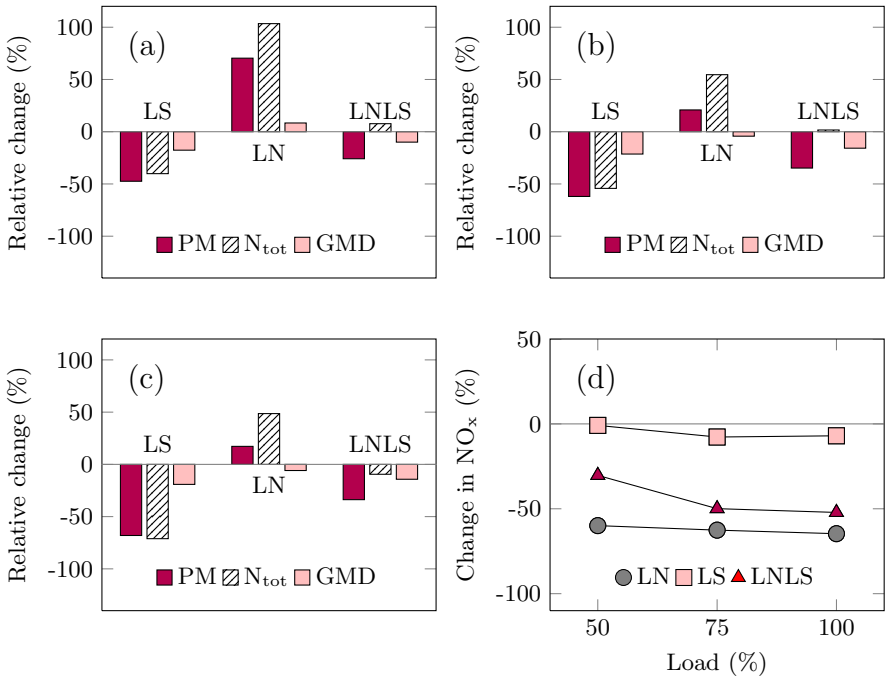

Figure 4.2: Relative changes in particulate (PM, number emission, GMD and FSN) on the (a) 50 % , (b) 75 % and (c) 100 % loads and (d) NO_x emissions due to engine parameter adjustments at the studied engine loads. The presented changes are relative to the emission at standard engine conditions with HVO fuel. Modified from **Paper 2**.

with this engine are only indicative. Especially the EGR values presented in Table 4.1 might not be representative to the real situation. The reason to this is that, in the study of **Paper 2**, the EGR was simulated by supplying neat nitrogen gas in the charge air. Zheng et al. (2004) reported that simulating EGR by adding neat CO_2 gas in engine intake simulates quite well the thermodynamic and dilution effects of EGR. Nevertheless, EGR simulated with gaseous add-ons is always pure from particulate matter contrary to actual recycled exhaust gases. As the use of EGR simulated with neat nitrogen should be quite close to the simulation by CO_2, nitrogen EGR should reproduce NO_x emission quite well but it may underestimate particle emissions. Thus, the conditions presented in Figure 4.2 might have produced higher particle emission if real EGR was used. Further, the engine model and technology will surely influence on the emission reductions obtainable by adjusting engine parameters for HVO fuel.

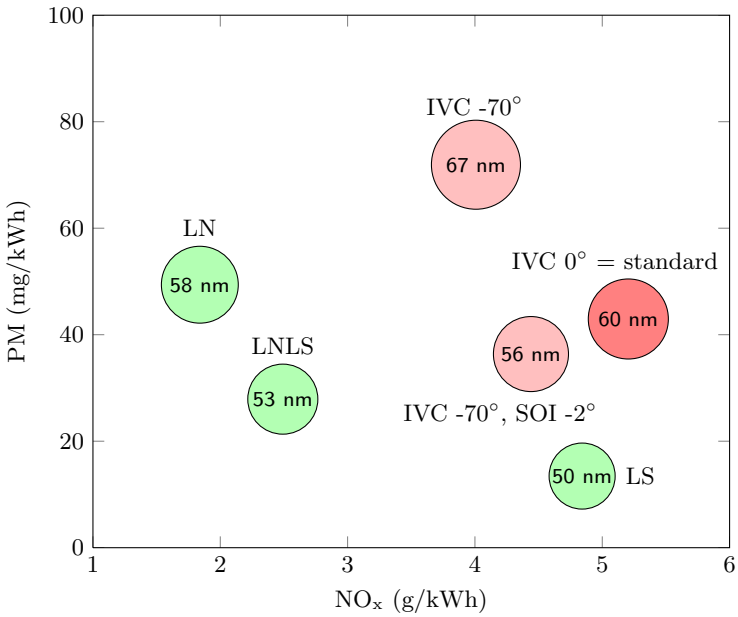

Figure 4.3: PM and NO_x emissions as well as GMDs of measured size distributions on the 100 % load. The emissions and GMDs of the LN, LS and LNLS conditions (green), the adjusted IVC -70 °CA conditions from **Paper 1** (pink) and the standard 100 % conditions (darker red) are presented.

4.2 Blended oxygenate

One method to improve the combustion process in an engine is to modify fuel composition through the addition of oxygenate. Oxygenates are essentially fuel components which contain oxygen. Many biofuels that are used in engines are thus in essence oxygenates. These biofuels include ethanol, methanol, DME and FAME (i.e. conventional biodiesel), for example.

Oxygen in fuel facilitates combustion and, thereby, reduces particulate emissions. One suggested mechanism is that, since the carbon bonded to an oxygen atom does not readily participate in soot formation, the amount of soot precursors formed during combustion is reduced (Eastwood 2008). In addition, oxygen may facilitate the oxidation of the soot that has been already formed (Lapuerta et al. 2008). Nevertheless, it should be noted that adding an oxygenate component to fuel may significantly change such properties of the fuel as, for example, cetane number, viscosity or heating values, which may further have an influence on the combustion process. NO_x emissions are also affected by the added oxygenate. Often the reduction of particulate is accompanied

with an increase in NO_x but NO_x emissions may also remain unchanged or reduce (McCormick et al. 1997; Wang et al. 2012).

From the extensive research conducted regarding the use of oxygenates to complement conventional diesel fuel, one of the more accepted results is that the mass of soot particulate seems to reduce in proportion to the mass of oxygen in the fuel (Eastwood 2008). Nevertheless, there is also evidence that also the molecular structure of the oxygenate affects soot suppression (Kitamura et al. 2001). In any case, the proportionality of oxygen mass to soot mass suggest that, at high enough oxygen content in the fuel, the soot emissions will completely disappear. This threshold oxygen content is frequently cited to be 30–40 wt-% (Eastwood 2008). However, with as low as 2 wt-% oxygen content in fuel, particulate mass has been observed to decrease 10–20 % depending on the added oxygenate (McCormick et al. 1997; Ren et al. 2008).

A large number of different compounds has been studied as potential oxygenates for diesel fuel (see e.g. Pecci et al. (1991)). However, the fact that oxygenates are generally polar compounds but fuel hydrocarbons are non-polar may lead to miscibility problems between the fuel and the oxygenate (Tilli et al. 2010). When choosing the oxygenate best suitable for HVO fuel, almost 140 possible oxygenate compounds were reviewed. The preliminary screening of the review was reported by Tilli et al. (2010). In **Paper 3**, the oxygenate was chosen according to the following criteria:

- Cetane number greater than 51
- Flash point above 55 °C
- Boiling point in the range of 180–340 °C
- Soluble in diesel fuel

The target for the oxygen content of the resulting blend was set to be 2–3 wt-%.

From this review, di-n-pentyl ether (DNPE) was chosen to be best suitable for blending with HVO fuel. For more information on the other candidates see **Paper 3**. The potential of DNPE to act as diesel oxygenate has been also reported elsewhere (Pecci et al. 1991; Murphy 1999, 2002; Marchionna et al. 2000; Martin et al. 1997). The cetane number of DNPE is high (103–153) and other properties are diesel-like. Oxygen mass content in DNPE is 10.1 wt-%.

In order to achieve a fuel blend with 2 wt-% oxygen, 20 wt-% DNPE was added to HVO fuel. The properties of the resulting blend as well as the corresponding properties of HVO fuel are presented in Table 4.3. As it can be seen from the table, the addition of oxygenate increased the cetane number of the fuel but decreased heat values and viscosity. Further, the addition of oxygenate also increased the HFRR lubricity value meaning that the lubricity of the fuel was decreased. It should be noted that neither the oxygenate reviewing process, the final selection of the oxygenate compound nor the choosing of the blending percentage were performed by the author of this thesis.

Table 4.3: Fuel properties of the studied HVO fuel and 80 % HVO + 20 % DNPE fuel blend. The studied HVO fuel included lubricity additive. Modified from **Paper 3**.

	HVO	80 % HVO +20 % DNPE
density 15 °C (kg/m^3)	779	781
viscosity 40 °C (mm^2/s)	2.985	2.348
higher heating value (MJ/kg)	47.216	46.25
lower heating value (MJ/kg)	43.991	43.137
cetane number	88.2	93.9
HFRR lubricity (μm/60 °C)	351	493

Table 4.4: Total particulate mass (PM), total particle number emission (N_{tot}), geometric mean diameter of the particle size distribution (GMD) and nitrogen oxide emissions (NO_x) of the engine at the 50, 75 and 100 % loads with standard engine conditions using HVO fuel. (**Paper 3**).

Load (%)	PM (mg/kWh)	$N_{tot} \cdot 10^{14}$ (#/kWh)	GMD (nm)	NO_x (g/kWh)
50	100	3.0	63	3.01
75	85	2.4	68	3.58
100	45	1.4	66	5.03

The study on the effects of HVO-DNPE blend on exhaust emissions was performed using the same single cylinder research engine that was used to study the effects of engine parameter adjustments (see Section 4.1). The particle size distributions measured with HVO and with 80 wt-% HVO 20 wt-% DNPE blend are presented in Figure 4.4. According to the measurements, the particle size distributions were all unimodal. Further, no indication of particles less than 10 nm in diameter was found. This is in line with previous measurements conducted with this engine. The particulate and NO_x emissions at standard engine conditions with HVO fuel for the three studied loads (50 %, 75 % and 100 %) are presented in Table 4.4.

When comparing Tables 4.2 and 4.4, it can be noted that the PM emission was essentially the same at these separate measurements. Further, the GMDs and the NO_x emissions were also quite similar to those measured previously. Particle number

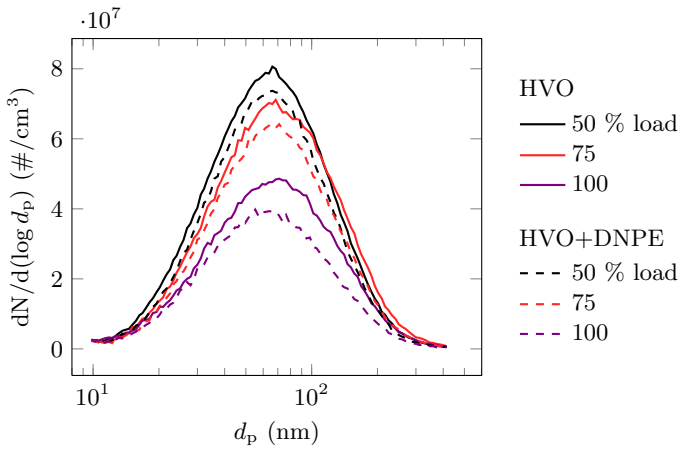

Figure 4.4: Particle size distributions measured with HVO and 80 wt-% HVO 20 wt-% DNPE blend used as fuel. Size distributions were measured on the 50, 75 and 100 % loads. Modified from **Paper 3**.

emission values, on the other hand, were over three times higher in Table 4.2 compared to the values in Table 4.4. This is caused by a small difference in the particulate measurement system between the two measurement campaigns. At the oxygenate measurements, an additional dilution was used before the CPC (CPC 3775, TSI Inc.) measuring the total particle concentration. However, although the additional dilution ratio was taken into account when calculating the particulate emission, the additional dilution resulted in a change in the counting mode of the CPC 3775. Thus, at oxygenate measurements of Table 4.4, the CPC operated in the single-particle counting mode whereas, at the measurements of Table 4.2, the CPC operated in the cloud counting mode. Thus, the discontinuity between the different counting modes is the most probable reason explaining the difference in the number emission values between the separate measurements at standard engine conditions.

Figure 4.5 presents the changes in particulate and NO_x emissions induced by the use of the HVO-DNPE blend compared to pure HVO fuel. The results show that the relative changes in emissions remain quite similar between the studied engine loads. Particulate mass was reduced 25–30 % and the total particle number emission 10–17 %. A decrease of 3 % and 7 % in the GMDs of the particle size distributions was observed on the 75 % and 100 % loads, respectively. On the 50 % load, the GMD was unchanged. However, even though the PM was reduced over 25 %, the simultaneous increase in NO_x emissions was below 5 % on all measured loads. In fact, on the 50 % load, the NO_x emission was actually decreased by 2 %.

Here, the observed decrease in PM is greater than the reductions reported by

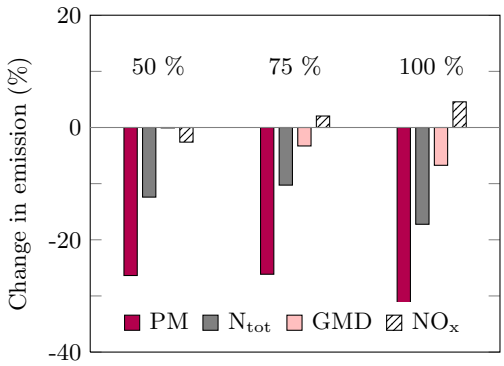

Figure 4.5: Relative changes in emissions caused by the use of 20 wt-% DNPE content with the HVO fuel on the 50, 75 and 100 % engine loads. Changes in particulate mass (PM), total number emission (N_{tot}), geometric mean diameter of the particle size distribution (GMD) and NO_x are presented. (**Paper 3**)

McCormick et al. (1997) and Ren et al. (2008) for fuel with 2 wt-% oxygen content. However, they used different base fuel (conventional diesel) and different oxygenate compounds in their study. Marchionna et al. (2000) studied the use of DNPE as oxygenate for conventional diesel with 10 wt-% and 20 wt-% blends. They reported that PM emission decreased by 15–20 % and NO_x 2–2.5 % due to the use of the blends. This reduction is in line with the reports on the effects of 2 wt-% oxygen content fuel that were mentioned earlier (McCormick et al. 1997; Ren et al. 2008) but the PM reduction was still somewhat lower than that obtained with 80 wt-% HVO 20 wt-% DNPE blend.

Nevertheless, all the above mentioned studies used conventional diesel fuel as the base fuel. An example of an oxygenate study with paraffinic diesel as base fuel was reported by Nabi and Hustad (2010). They blended jathorpa biodiesel to Fischer-Tropsch diesel and reported a 34 % decrease in smoke emissions with a blend containing 2.825 wt-% oxygen. The agreement between this result to the results presented in Figure 4.5 depends on the amount of volatiles in the PM results of this thesis. However, the reduction of smoke could be in line with the PM reduction of this study as the OC/EC analysis presented later on (Figure 5.12) indicates.

Gill et al. (2011b) studied conventional diesel with added oxygenate (biodiesel and diglyme) and reported that, in addition to PM, also particle number concentration decreased with increased oxygen content in the fuel. This result is in line with the results in Figure 4.5 which show the decrease in particle number concentration also. The decrease in number concentration may partly explain the observed decrease in

GMD as the reduced particle number concentration suppresses particle growth by coagulation.

Both increases and decreases in NO_x emission due to oxygenated fuel have been observed depending on the added oxygenate (McCormick et al. 1997). Often not only the presence of oxygenate in fuel but also the amount of blending affects NO_x emissions (Wang et al. 2012; Nabi and Hustad 2010). Further the results in Figure 4.5 show that also engine load affects the changes in NO_x emissions. However, all the changes in NO_x emissions were quite small (below 5 %) compared to the particulate emission reductions.

4.3 Discussion of the results

In this chapter, it has been shown that the exhaust emissions of a HVO-fueled engine can be further decreased by utilizing engine parameter adjustments or by adding oxygenate to the fuel. The engine parameter adjustments tested in this thesis involved the appliance of Miller timing together with an increase in fuel injection pressure. The appliance of Miller timing requires an increase in the intake air pressure. This may be a bottleneck for some of the engine-early IVC combinations as the boost pressure required by Miller timing could be higher than the practical boost pressures obtainable with superchargers (Benajes et al. 2009a). However, in this thesis the maximum intake boost pressure was 3.9 bar which is well below the attainable boost pressure with a two stage turbocharged engine reported by Benajes et al. (2009a). Thus, the applicability of Miller timing depends on engine technology in this respect.

In addition to high intake pressures, the realization of Miller timing requires also variable valve timing. Variable valve actuator (VVA) systems are in quite widespread use in gasoline engines. Nevertheless, there are some issues that hinder the increasing frequency of VVA for diesel engines. First, the VVA systems are more complex than current production systems and, second, the VVA systems do not increase the efficiency and performance of the diesel engine in the extent they do in gasoline engines (Lancefield et al. 2000). Thus, the more common use of VVA systems in diesel engines depends primarily on emission legislation and on customer related matters (Lancefield et al. 2000).

The applied elevated injection pressures in this thesis (600–1400 bar) are most likely applicable for a heavy-duty engine. At least, they were in the range of the study of Lähde et al. (2011) where the effect of injection pressure on the particle size distribution was studied with a 6-cylinder heavy-duty off-road engine.

With the engine parameter adjustments, it was possible to decrease either PM emission 45–68 % or NO_x emission roughly 60 % depending on load. It must be remembered that the emission reduction percentages are strongly depended on applied

engine technology and aftertreatment systems but similar trends in emissions can probably be obtained also with different engine models. Nevertheless, at least with the current strictening limits for particles, it is practically impossible that light duty vehicles or heavy-duty engines could achieve these limits without the use of particulate filters (DPF). However, by adjusting the engine to reduce NO_x emission, separate NO_x aftertreatment (i.e. SCR) could possibly be avoided.

From the measurements, it becomes evident that engine performance with HVO fuel can be improved by adjusting engine parameters. Nevertheless, it is not probable that these kind of parameter adjustments ever become common in serial production engines. As discussed by Aatola et al. (2008), the full benefits of the HVO fuel could be realized in dedicated centrally fueled vehicle fleets which could have their engines optimized for the HVO fuel.

The use of oxygenated HVO fuel could also be most beneficial in centrally fueled vehicle fleets. Even though the use of DNPE oxygenate decreased exhaust PM emissions considerably (25–30 %), the reduction is by no means enough to enable engine operation without a DPF aftertreatment with the current PM emission legislation. However, the use of oxygenate would probably provide more margin to the use of EGR to further reduce NO_x emissions of the fleet's engines.

Furthermore, the choosing of DNPE as the oxygenate for HVO fuel was decided by considering only the technical aspects and the availability of the oxygenate for the tests. That is, the price of the oxygenate was not considered. Nevertheless, after the technical suitability, the price is probably the most important property of the oxygenate determining its applicability to more widespread use. Thus, even though DNPE is probably technically one of the best oxygenates available for HVO fuel, it is to be expected that, in near future, the more widespread use of oxygenate together with HVO fuel starts from a cheaper oxygenate, for example from FAME biodiesel.

Chapter 5

Effect of fuel on particle surface

5.1 Studied properties

The nanoparticles emitted by different fuels during combustion may have differences in their chemistry and structure. These differences may show as differences in the behaviour of particles in aftertreatment devices, the atmosphere or in the human respiratory system. Often, the behaviour of particles in different environments is also linked to surface properties of the particles, such as hygroscopicity and oxidizability.

In this thesis, particle microstructure, oxidizability and hygroscopicity of emitted diesel exhaust particles are studied in the context of HVO fuel. The studying of surface fine structure together with other surface properties of particles is important since the fine structure may explain some of these properties. For example, it is known that rougher surface and, thereby, higher specific surface area facilitate nanoparticle oxidation (Su et al. 2004b). Vander Wal and Tomasek (2003) even reported that the wide range of oxidation rates of soot reported in literature may possibly be caused by differences in the initial nanostructures of the studied soot particles.

The oxidizability of soot particles is important for two reasons. First, the oxidation properties of soot particles affect vehicle exhaust especially in the vehicles equipped with particulate filters. The reason is that the regeneration of these filters are performed by oxidizing the soot deposited on the filter surface (Konstandopoulos and Kostoglou 2000). Thus, the oxidizability of soot particles affects the reliability of the filters and, further, on the counterpressure caused by the filters, i.e., on fuel consumption. The second reason is that particles having higher oxidizability often also have higher overall reactivity. The overall reactivity, on the other hand, increases particles' cytotoxicity (Su et al. 2008) and, thereby, their adverse health effects.

Hygroscopicity describes particles' ability to grow by adsorption or absorption of water vapour. It affects the deposition of particles in the human respiratory track and the light scattering of particles and, thereby, visibility as these properties are strongly particle size dependent. Moreover, hygroscopicity influences on the ability of emitted particles to act as cloud condensation nuclei and, thus, it affects particles'

interactions with clouds. The addition of water in the atmosphere may also alter several chemical and physical properties of the particles such as acidity, amount of water soluble condensates, chemical reactivity, particle size, mass and optical properties.

5.2 Particle microstructure

The structure of soot particles emitted using HVO fuel was studied with a high resolution transmission electron microscope (HR-TEM) in **Paper 4**. The particles were produced with a turbocharged 6-cylinder direct injection heavy-duty diesel engine meeting the European Stage III A emission standard. The particles were sampled with a single heated ejector diluter followed by a thermodenuder. The temperature of the heated dilution air as well as the temperature of the thermodenuder was 200 °C. The collection was conducted on the 50 % and 100 % engine loads.

The HR-TEM sample collection was performed by first charging the particles with a corona charger and then using an electric field to deposit the particles on holey carbon coated copper TEM grids. The holey carbon coated copper grids were used in order to be able to image the particles without the interference from the underlying TEM grids. This is possible for the particles that are collected on the edges of the grid's holes in a way that they are protruding over the holes.

TEM images of the measured soot particles produced with both HVO and conventional EN590 diesel fuel on the 50 % load are presented in Figure 5.1. In general, the soot particles were agglomerates consisting of primary particles having an average diameter of 26 (±4) nm. There was practically no difference in the average size of the primary particles between different engine conditions and fuels. High resolution TEM images on the 100 % load are presented in Figure 5.2 and, on the 50 % load, in Figure 5.3. No notable differences were observed between the soot particles collected on the two loads. Figure 5.2 shows that soot particles were formed from strongly bent graphene layers which resulted in an "onion" like structure of soot. Near the center of the primary particles, graphene layers were more strongly bent and, thus, the structure appears less ordered. From some of the primary particles, it could be seen that they included multiple structural nuclei. According to Su et al. (2004b), the multiple nuclei are caused by the strong bending of the graphene layers.

As seen in Figure 5.3, the outer surfaces, i.e. the edges of the particles, were quite rough. In general, rough outer surface induces greater reactivity than smooth surface since the rough surface includes a greater amount of non-completed carbon rings to which additional molecular oxidants may bond (Su et al. 2004a,b). It appears that the soot particles produced using HVO might have slightly rougher surface than those produced using conventional diesel, but the difference is quite small.

In order to obtain a quantitative point of comparison, the distances between

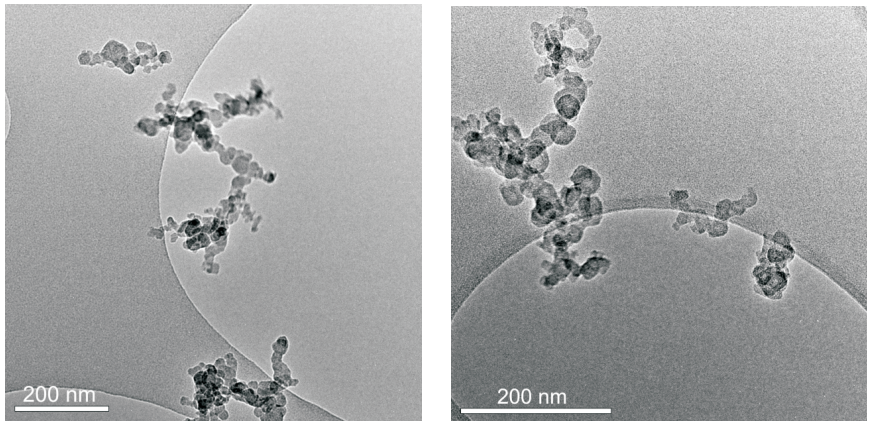

(a) HVO (b) EN590

Figure 5.1: TEM images of soot particles produced with HVO (a) and with conventional EN590 diesel (b) as fuel on the 50 % load 2200 rpm engine conditions.

the graphene layers were measured from HR-TEM images of both engine conditions. The average distances were obtained by measuring line profiles across the fringes of graphene layers on 5–6 places on different images (Figure 5.3). The results for the average distances were 3.76 (±0.19) Å for the HVO and 3.63 (±0.19) Å for the conventional diesel. It should be noted that the observed distances between the graphene layers are greater than the distance between the layers in graphite which is 3.362 Å (Müller et al. 2005). Thus, the distances between the graphene layers of soot particles were very similar between the fuels which strengthens the conclusion that soot particles were structurally very similar.

In addition to HR-TEM images, also electron energy loss spectra (EELS) were obtained from the soot particle samples. The EELS were acquired from samples produced with both fuels on the 100 % and on the 50 % engine loads. An EELS spectrum is an energy spectrum of electrons that have traveled through the sample particle. These electrons may have lost no energy or they may have suffered inelastic collisions in the sample particle (Williams and Carter 2009). The energy loss events provide information about the chemistry and the electronic structure of the atoms in the sample particle. In order to avoid misinterpretations of the energy loss, all the spectra were acquired from the sample particles protruding over the holes of the underlying carbon film.

The electron energy loss near-edge structures (ELNES) from the EELS spectra of the carbon K ionization edge of soot particles with different fuels are presented in

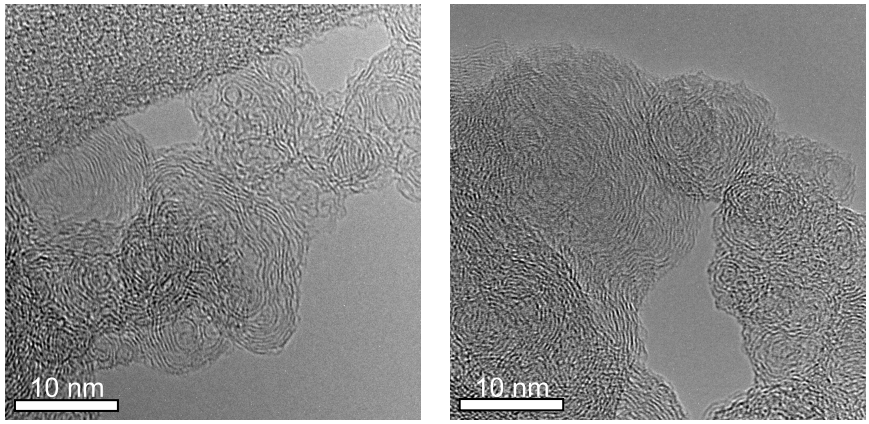

(a) HVO (b) EN590

Figure 5.2: HR-TEM images of soot particles produced with HVO (a) and with conventional EN590 diesel (b) as fuel on the 100 % load 2200 rpm engine conditions. (**Paper 4**)

Figure 5.4. According to the ELNES presented in the figure, the soot particles of both fuels are graphite-like, but no clear differences between the soot particles could be found either in the first peak of the ELNES, corresponding to double bonds (1s–π^* transitions), or in the second peak, corresponding to single bonds (1s–σ^*). However, the soot samples differed from the ELNES of the TEM grid carbon film especially in the respect of the higher first peak in the spectra of soot particles. Thus, the study of EELS spectra of soot particles led to a conclusion that the soot samples produced with different fuels were similar in microstructure, but that structure deviated from the structure of graphite.

5.3 Oxidizability

In this thesis, a tandem differential mobility analyzer (TDMA) measurement technique was applied for studying oxidizability of soot particles. As the same general technique was used also in studying hygroscopicity, and as the building of the TDMA apparatuses has been a major part of the thesis work, it is worth to provide here a short introduction to TDMA techniques in general.

Originally, the TDMA technique was introduced by Liu et al. (1978) to study sulphuric acid aerosols. A schematic of the technique is presented in Figure 5.5. The principle is to use a differential mobility analyzer (DMA) to first classify particles to obtain a sample of a chosen electrical mobility diameter and then to use sample

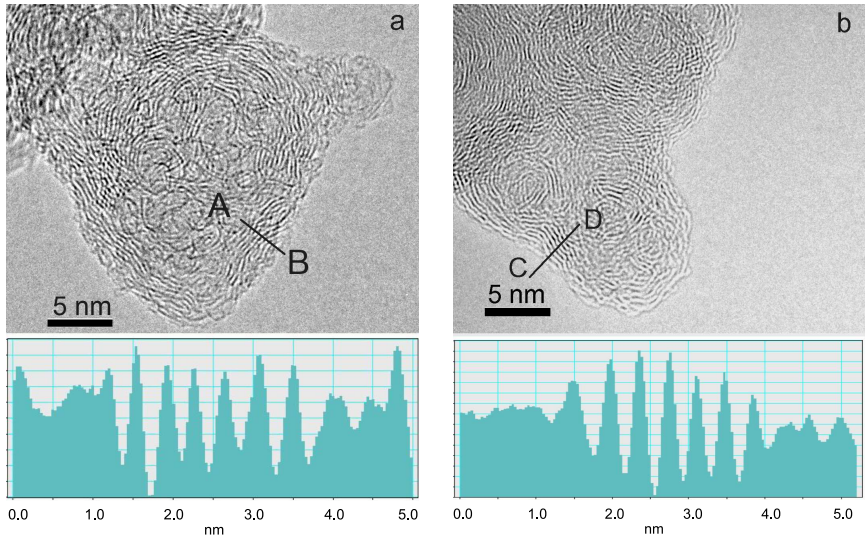

Figure 5.3: HR-TEM images of a sample HVO (a) and a sample conventional EN590 diesel (b) particle measured at 50 % 2200 rpm. Line profiles along A–B and C–D, 30 pixels wide, indicate very similar distances between graphene planes (in this measurement 0.366 and 0.386 nm respectively). (**Paper 4**)

conditioning to potentially impose changes to the mobility diameter of the classified particles. Finally, the size distribution of the resulting sample aerosol is measured with another DMA followed by a particle counter. From measurements through and bypassing the conditioning, information about the properties of sampled particles can then be obtained. The applied conditioning can be humidification (e.g. Liu et al. 1978; Rader and McMurry 1986; Hennig et al. 2005), humidification and subsequent drying (e.g. Weingartner et al. 1997), humidification via ethanol vapour (Joutsensaari et al. 2001) or furnace treatment (e.g. Higgins et al. 2003). The TDMA technique can also be used to measure the charge distribution of aerosol particles by installing a bipolar charger as the conditioner (Kim et al. 2005). In this thesis, the TDMA technique has been applied to study oxidizability and hygroscopicity of exhaust particles. More detailed descriptions of the actual TDMA measurements systems applied to study these properties can be found in the corresponding sections of this chapter.

It has been shown that, in addition to the engine conditions and technology, also the applied fuel affects the oxidation properties of diesel soot particles (Jung et al. 2006). Thus, it was worth studying whether there exists a difference in oxidizability between the particles produced using HVO fuel compared to those produced using

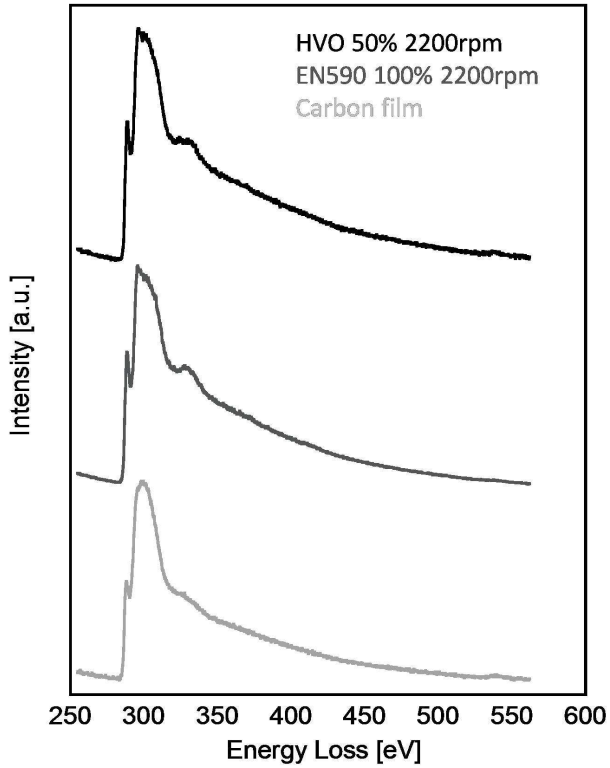

Figure 5.4: ELNES of the carbon K ionization edge of HVO soot (black), conventional EN590 diesel soot (dark grey) and, for comparison, the ELNES of the TEM grid carbon film (light grey). The HVO soot was collected on the 50 % load and the EN590 soot on the 100 % load. (**Paper 4**)

conventional EN590 diesel fuel. Oxidizability of HVO and conventional diesel produced soot particles was studied with a heavy-duty diesel engine (see **Paper 4** for engine and fuel details).

The TDMA measurement system applied for studying oxidizability in this thesis is presented in Figure 5.6. Particle sample was first diluted by an ejector diluter having a dilution ratio (DR) of approximately 10. The dilution gas for the ejector diluter was heated to 200 °C in order to prevent the condensation of volatiles on the particles during the dilution. The removal of volatiles was later ensured by having the sample treated with a thermodenuder.

After the thermodenuder, the sample line split to two branches (Figure 5.6). The first branch continued with a secondary ejector diluter (DR≈10). In this branch, there was an electrical low pressure impactor (ELPI) to monitor the stability of the particle

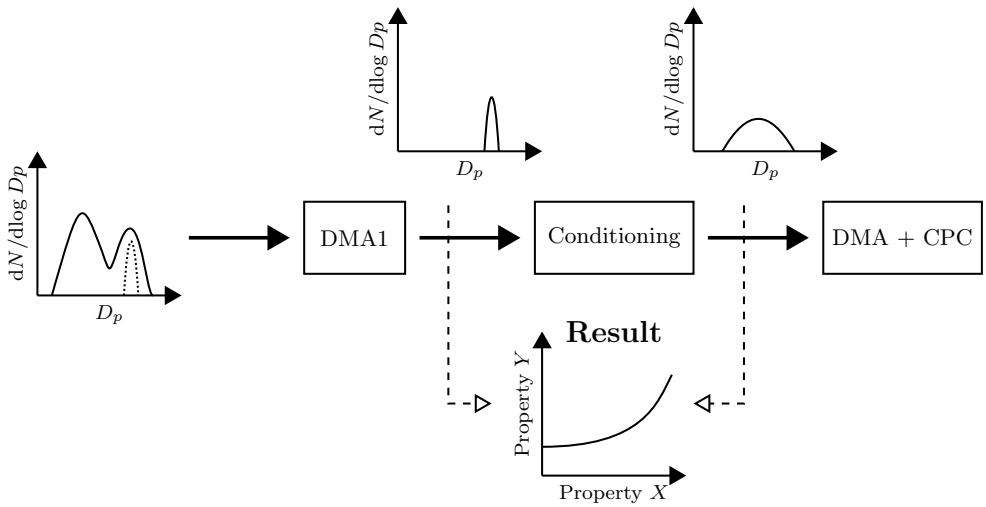

Figure 5.5: A schematic of the TDMA technique.

sample and an NO_x analyzer that was used to monitor the dilution ratio.

The second branch consisted of a so-called high-temperature oxidation TDMA (HTO-TDMA). The HTO-TDMA technique was introduced by Higgins et al. (2002) and, since then, it has been successfully applied, for example, by Higgins et al. (2003), Jung et al. (2006) and Shrivastava et al. (2010). In the HTO-TDMA system, as in TDMA systems in general, a narrow particle size distribution of a chosen particle size is first classified with a DMA after which the size distribution is subjected to conditioning. The conditioning in the case of HTO-TDMA is a high temperature treatment in a furnace. The function of the furnace was to heat the classified aerosol to so high temperatures that particle oxidation would further proceed. After the oxidation, the resulting particle size distribution was measured with a scanning mobility particle sizer (SMPS). The oxidation was measured by measuring the particle size reduction in the high temperature furnace. In order to estimate the significance of possible non-oxidative particle size reduction, the carrier gas of the particle sample was changed to non-oxidative gas by selecting nitrogen as the sheath gas of the first DMA. The measurement system also allowed bypassing the furnace, the first DMA or both.

In earlier studies, the HTO-TDMA technique has been applied in determining the oxidation kinetics, especially activation energy, of soot generated by an ethylene flame (Higgins et al. 2002) and a diesel engine (Higgins et al. 2003; Jung et al. 2006). Higgins et al. (2003) reported that the oxidation of exhaust soot particles is more pronounced on the 10 % load than on the 50 % or 100 % load. Further, Jung et al. (2006) studied the oxidation of soot emitted by an engine run with 100 % soy methyl ester biodiesel as

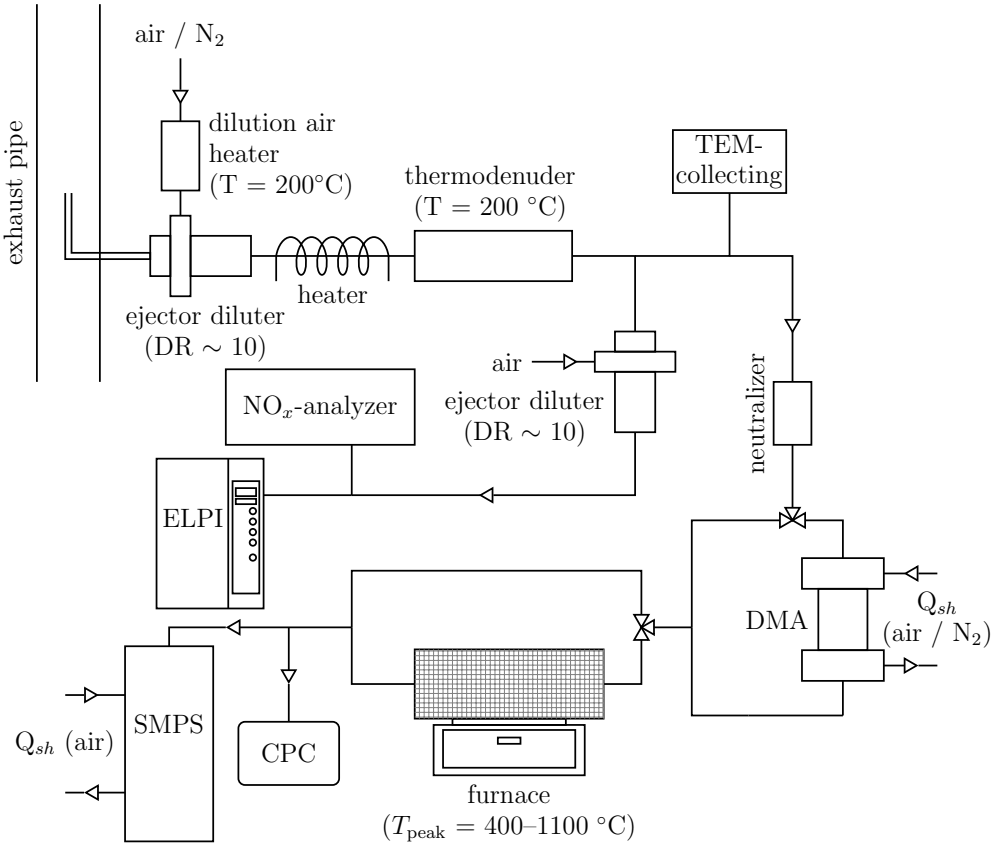

Figure 5.6: Measuring system for studying the oxidizability of soot particles. (**Paper 4**)

fuel and observed that such particles are more readily oxidized than conventional diesel generated particles. In the oxidation study of **Paper 4**, no emphasis was given to finding kinetic parameters of oxidation contrary to the mentioned earlier HTO-TDMA studies as the study was focused on the comparison of oxidation behaviour and surface properties between conventional EN590 diesel and HVO produced soot particles.

An example of size-selected particle size distributions measured through the furnace are presented in Figure 5.7. The original dry particle size classified by the first DMA was 83.3 nm. It can be observed from the figure that as the furnace temperature increased, the particle concentration as well as the GMD of the particle size distribution decreased but the distribution became wider. The reduction in particle concentration is mainly caused by thermophoretic losses that occur during the cooling of the aerosol sample after the furnace. The widening of the distribution, on the other hand, is most probably caused by the wide distribution of particle residence times in the furnace

(Higgins et al. 2002).

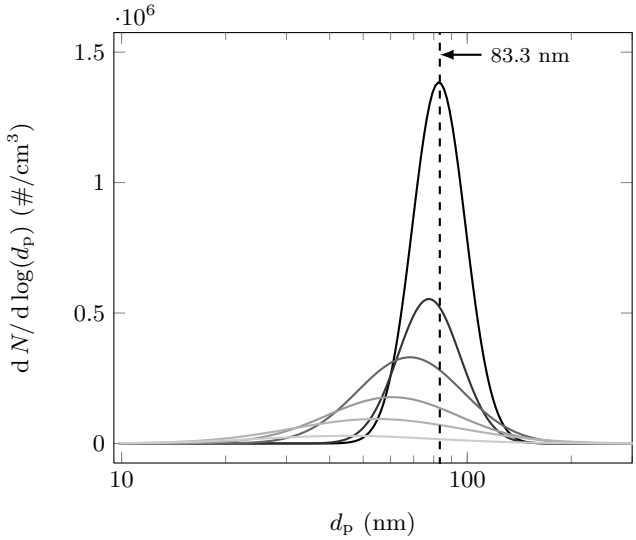

Figure 5.7: Lognormal distributions fitted to the measurements through the classifying DMA. The furnace peak temperatures from the darkest distribution to the lightest are 25, 744, 844, 894, 944 and 994 °C. The fuel was fossil EN590 diesel and the original particle size selected by the classifying DMA was 83.3 nm. (**Paper 4**)

The chosen particle size (83.3 nm) was situated roughly at the GMD of the particle size distribution measured on the 50 % load at 1500 rpm engine speed. The oxidation measurements were also conducted in the 100 % load 1500 rpm engine conditions. Particle size distributions at these loads are presented in Figure 2 of **Paper 4**. A lognormal distribution was fitted to each SMPS particle size distribution measurement in order to obtain an accurate value for the GMD of the distribution.

Figure 5.8 presents the furnace treated mean particle sizes of monodisperse 83.3 nm soot particles as a function of furnace peak temperature. In the results of Figure 5.8(a), pressurized air was used as the carrier gas for the soot particles, whereas, in Figure 5.8(b), the carrier gas was nitrogen. As it can be seen from Figure 5.8(b), particle size starts to reduce in the furnace even without oxygen. The particle size reduction without oxygen in the carrier gas cannot, of course, be oxidation. The reason of the reduction cannot be further evaporation of volatile condensed species either since the particle size decrease did not start until the furnace temperature reached 700 °C. Further, the evaporation of volatile matter should only cause small changes in particle diameter since for, agglomerate particles such as soot, a major proportion of the condensated volatile matter fills the voids of the agglomerates. Thus, the reason for

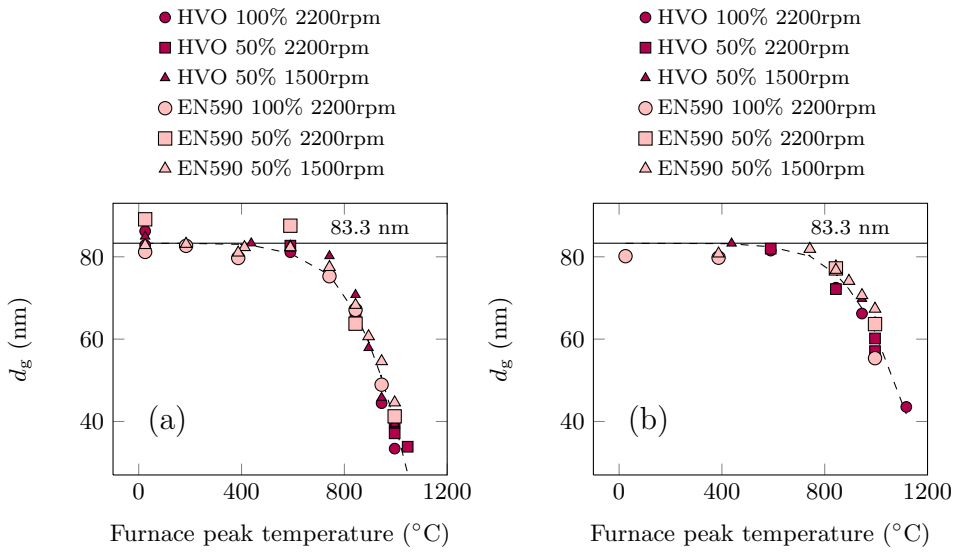

Figure 5.8: GMD of monodisperse (83.3 nm) diesel soot particles after furnace treatment as a function of furnace peak temperature. Pressurized air (a) and nitrogen (b) were used as the carrier gas for the particles. Modified from **Paper 4**.

this size decrease is most probably non-oxidative particle restructuring, i.e. sintering. Particle size reductions having nitrogen as the carrier gas have been also observed before (Higgins et al. 2002, 2003) although the reductions have been lower than in **Paper 4**. As it can be seen from Figure 5.8(a), the particle size reduction was over 20 nm at 1000 °C. In previous studies (Higgins et al. 2002, 2003), the non-oxidative particle size decrease has been 11 nm at most (Higgins et al. 2003) but usually only few nanometers.

However, when pressurized air was used as the carrier gas (Figure 5.8(a)), the particle size decrease was more pronounced. This indicates that further particle oxidation occurred. In all the measurement situations with pressurized air, the mean particle size remained at 83 nm until the furnace peak temperature reached approximately 750 °C. On higher temperatures, particles started to decrease reaching almost 50 nm decrease in particle size at approximately 1000 °C furnace peak temperature. However, the main result presented by Figures 5.8(a) and 5.8(b) is that there was no observable difference in the behaviour of the mean particle size as a function of the furnace peak temperature between the measurements performed with different fuels in different engine conditions. The result indicates that soot particles had similar oxidation characteristics in all the studied measurement situations.

All in all, the oxidation results presented above support well the particle structure results presented in Section 5.2. Both results conclude that there are no major chemical or structural differences between the soot particles generated with HVO and with conventional diesel. With the current setup, the temperature range of the oxidation measurements is limited by the amount of aerosol particles in the sample. The reason to this is that, at high furnace temperatures, the thermophoretic losses occurring during the cooling of the aerosol increase strongly with increasing temperature. Moreover, the increased losses at high temperatures occur together with the widening of the particle size distributions thus decreasing the accuracy of the determination of the GMD.

5.4 Hygroscopicity

Particle hygroscopicity was studied with a hygroscopic TDMA (HTDMA) in which the particle sample is conditioned by exposing it to high relative humidities. Already the first TDMA system of Liu et al. (1978) was essentially a HTDMA setup and, since then, several improved HTDMA setups have been built and reported (e.g. Rader and McMurry 1986; Weingartner et al. 1997, 2002; Hennig et al. 2005; Johnson et al. 2008). HTDMA systems produce particle growth factors as a function of relative humidity as the output. Particle growth factors are ratios of particle sizes between the humidified and the non-humidified, i.e. unconditioned, particles.

The HTDMA system applied in this thesis is presented in Figure 5.9. After selecting the particle size with the first DMA (DMA1), the sample is led to an insulated chamber enclosing the humidification system and the second DMA (DMA2). The sample is first humidified in a Nafion humidifier and then measured with DMA2. The sheath air of DMA2 is also humidified in order to hinder the sample from evaporating or taking on more water due to the difference in relative humidities between the sample and sheath flows.

The humidity conditioning in the system is performed on two stages. A pressurized air flow is first humidified with water in order to obtain an air flow having close to 100 % relative humidity (RH). The temperature of the moisturizing water is controlled with a water bath capable of adjusting water temperature. The flow of high RH is then diluted with another flow of pressurized air to reach the humidity chosen by the operator. Next, the humidified air and the sample aerosol are conducted to the Nafion humidifier where the humidity between the two flows is balanced and, thus, the sample flow is humidified. The Nafion humidifier only transfers water from the humid flow to the drier one but it does not mix the flows. After balancing the humidity, the humidifying air flow is then used as the sheath air flow for DMA2.

In the HTDMA system, temperature and humidity are monitored with five combined humidity and temperature sensors. One of these sensors (the uppermost in Figure

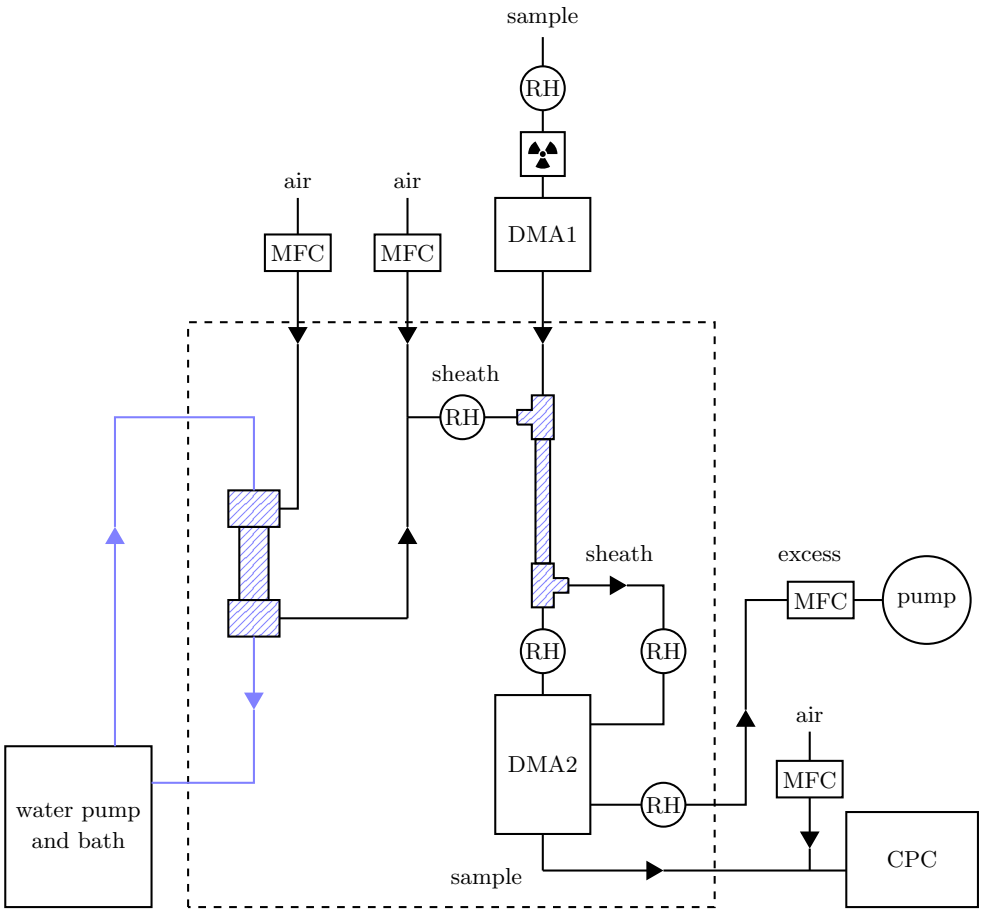

Figure 5.9: HTDMA setup. Blue lines represent water lines and black lines sheath air/sample lines. The humidifiers are marked with blue patterns. The dashed line represents the insulated chamber enclosing the DMA2 with the humidity control. (**Paper 3**)

5.9) monitors that the aerosol entering the system is dry enough, i.e. no significant hygroscopic growth had occurred before the HTDMA. Further, two of the sensors measuring temperature and humidity of the sheath and sample flow monitor whether the humidities of the flows had balanced in the Nafion humidifier so that no significant particle size change due to evaporation or condensation should occur within DMA2. However, the most important humidity sensor is the one measuring the humidity of the DMA2 excess flow, i.e. the humidity at which the growth factors are reported in the measurement results. In addition to these sensors, there was also a temperature and humidity sensor monitoring the sheath air flow before the Nafion humidifier. This sensor was important at the developing stage of the system as it monitors the humidity obtained by mixing the dry and humid pressurized air flows.

The design of the HTDMA system shown here was chosen to enable the field use of the devise in different emission measurement campaigns. Therefore, the focus of the design was on portability and on fast RH adjustment. The humidity adjustment by mixing a nearly water saturated air flow with a dry air flow allowed the said fast RH adjustments. The time needed for the adjustment of humidity is mostly limited by the adaptability of the Nafion humidifier to the changed conditions. Also, the HTDMA sample had the capability to bypass the Nafion humidifier although it is not shown in Figure 5.9. Thus, by bypassing the Nafion humidifier with the sample flow and by providing the sheath flow as dry pressurized air, it is possible to reach dry conditions for measuring the dry particle size very quickly (≈1 min). Also the recovery from dry conditions to humid conditions is quite fast (≈5 min) since there are no flows through the humidifiers during the measurement of the dry particle size. A picture of the actual HTDMA system in its current form (in July 2012) is presented in Figure 5.10. The additional layer of insulation (the pinkish layer in Figure 5.10) and the Peltier cooler have been installed to the system after the measurements of **Paper 3**.

The size change of exhaust particles caused by water uptake was measured for two particle sizes (20 and 50 nm) for both HVO fuel and the HVO–DNPE blend discussed in Section 4.2. The 50 nm particle size situated 10–15 nm below the GMD of the exhaust particle size distributions (see Figure 4.4). The measured growth factors are presented in Figure 5.11. The particle sample was obtained with the porous tube sampling presented earlier in Figure 2.2. Thus, the particle sample contained both soot particles and the possible condensated species. The humidity error bar in Figure 5.11 represents the standard deviation of the temperature and humidity sensor reading during the measurement. The error bar of the growth factor, on the other hand, is calculated from the standard deviations of the measured GMDs of particle size distributions.

It should be stressed, however, that the results in Figure 5.11 cannot be taken as accurate quantitative results. The reason to this is that the applied system had no active temperature control at the time of the measurements so the temperature control

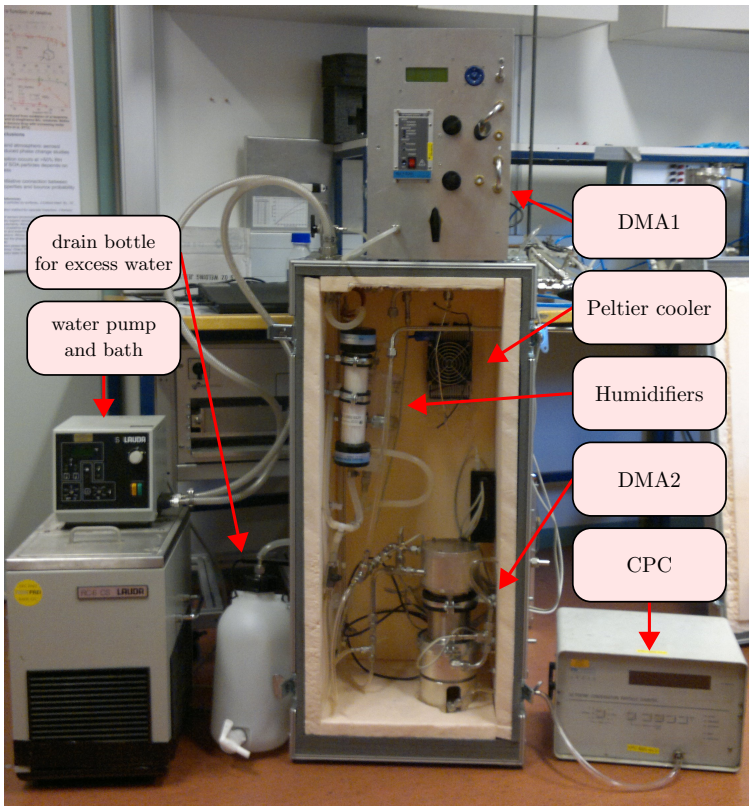

Figure 5.10: HTDMA system in its current form (July 2012).

relied only on insulation. This proved to be insufficient to remove temperature gradients from the system. There was a shift of 0.5 to 5.5 % RH between the sheath and sample flow entering DMA2, the sample flow having higher humidity in all cases. Further, there was a temperature drop between the sample flow and DMA2. This caused flow temperature to reduce 1.6–2.9 °C within the DMA causing 2–5 % RH increase in humidity. However, the measured humidities at the excess flow were very repeatable with both fuels, see the error bars of RH in Figure 5.11 showing the standard deviation. Although the absolute values of RH had large uncertainties, the uncertainties were quite systematical and, thus, allowed to study the results qualitatively.

The results show that hygroscopic growth of the measured particle sizes was very low (<2 % at roughly 90 % RH) with both studied fuels. The low growth factors are in line with Weingartner et al. (1997) who measured the growth factors for fresh soot particles of roughly 1.01 for 50 nm particles at 90 % RH. Further, it seems that 50 nm particles have slightly lower growth factors than 20 nm particles. This is to be

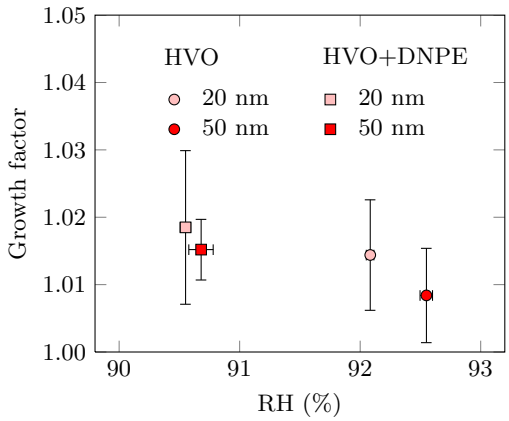

Figure 5.11: Particle growth factors as a function of relative humidity with two fuels (HVO and HVO+DNPE) and with two initial particle sizes (20 and 50 nm). (**Paper 3**)

expected since larger soot particles are more agglomerated and, thus, their more porous structure can hold more water without influencing the observed particle size. It has even been reported that large agglomerates may actually decrease in particle size due to the compaction of particles caused by the absorbed water (Weingartner et al. 1997; Henning et al. 2012).

According to Figure 5.11, the average values of measured growth factors are slightly higher with 80 % HVO and 20 % DNPE blend than with pure HVO fuel. However, the growth factors of particles emitted with HVO fuel were measured at approximately 2 % RH higher relative humidity. In general, the hygroscopic growth factor curves are exponential in their shape (e.g. Weingartner et al. 1997) so that higher humidities result in larger growth factors. Thus, the growth factors measured with HVO-oxygenate blend should have been even larger compared to those measured with HVO if the measurements had been conducted in exactly the same relative humidity.

The particle composition was further studied by determining the ratio between organic carbon (OC) and elemental carbon (EC) from filtered samples. In the applied thermal optical analysis method (Birch and Cary 1996), a sample of filtered exhaust gas is first heated in an oxygen-free atmosphere after which the amount of evaporated carbon (OC) is measured. After that, the sample is further heated in a helium/oxygen atmosphere while measuring the released carbon thus obtaining EC and pyrolysed OC.

The results of OC/EC-ratios in the samples are presented in Figure 5.12. As it can be seen, the amount of total carbon (OC+EC) decreases when the fuel is changed from pure HVO to HVO-oxygenate blend. However, this decrease is mainly caused by the decrease in the EC fraction. Overall, the OC fraction decreases less than 15 %

while the EC fraction loses roughly a third of its mass due to fuel change. This leads to higher OC/EC ratios for particles produced with HVO-oxygenate blend.

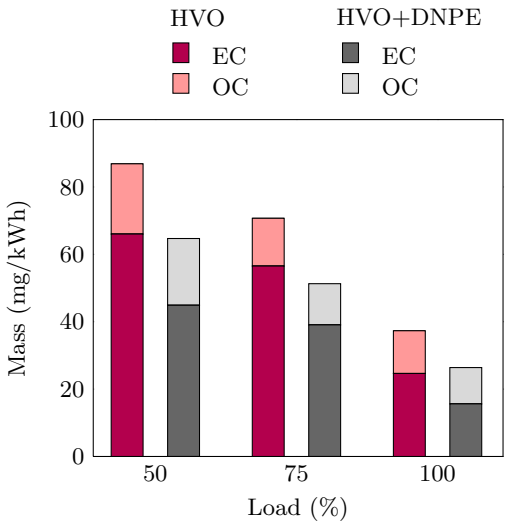

Figure 5.12: The fractions of organic carbon (OC) and elemental carbon (EC) in the total filtered particle mass. (**Paper 3**)

The result indicates that the slight increase in hygroscopicity might be caused by the somewhat larger amount of condensated organic species on the particles emitted with HVO-oxygenate blend. The higher OC content of particles may help to fill the cavities in the agglomerated structure of fresh exhaust particles. Therefore, less water might be required for "oxygenated particles" than for "HVO particles" to grow by a certain growth factor. Thus, in the view of the OC/EC results, it is possible that there are slightly more oxygen groups in particles emitted with the HVO-oxygenate blend and that they might contribute to the overall hygroscopicity but their contribution is very low.

Overall, there was a difference in hygroscopic growth of particles between the different fuels but the difference was small. As the hygroscopic growth factors of fresh particles emitted with both fuels were generally very low, it is improbable that the choice of fuel between HVO and HVO-DNPE blend significantly affects the behaviour of emitted exhaust particles in the atmosphere.

5.5 Discussion of the results

Generally in this study, there were no major differences between the surface properties of particles emitted with different fuels. One question arising from this result is that

how large differences are in fact observable with the applied measurement techniques. It is possible that the applied TDMA techniques are not very sensitive to the studied particle properties due to the agglomerated nature of exhaust particles. The oxidation measurement may suffer from the dominance of sintering in the particle size reduction and, as discussed earlier, the hygroscopic growth of agglomerates is masked by the water filling the cavities within the agglomerates.

Fortunately, in the case of studying oxidizability, the TDMA measurements were not the only measurements conducted. There was also the microstructure analysis together with the EELS analysis which agreed with the oxidation results regarding the similarity of the studied soot samples. Nevertheless, also with the TEM analyses, it can be difficult to find clear enough qualitative differences to distinguish between soot samples from different sources. Fortunately, there are some quantitative analyzing methods such as the lattice fringe analysis (Vander Wal et al. 2004), quantitative micro-Raman spectroscopy (Knauer et al. 2008) or calculations of the distances between graphene layers (**Paper 4**) which can facilitate the comparison of different samples. Nevertheless, these numerical analyses have to be conducted for a large enough number of individual particles in order to have adequate statistics.

Overall, the surface property results seem to indicate that changing the fuel from conventional diesel to HVO to HVO-DNPE blend should induce no major differences for the behaviour of exhaust particles in aftertreatment devices, the respiratory track or in the atmosphere. Thus, as a result of this thesis, the surface properties of particles produced with HVO should be no great concern when assessing the suitability of the fuel for wider use.

Chapter 6

Summary and final remarks

Stricter emission regulations, the ongoing global warming and concerns about the sufficiency of oil resources are all factors that promote the research and utilization of fuels from renewable feedstocks. This thesis has focused on one promising renewable fuel, diesel produced by hydrotreating vegetable oils (HVO), and studied it from the perspective of engine exhaust emissions. The thesis discussed the effect of HVO fuel on exhaust emissions (**Paper 1** and **Paper 4**) and the techniques to further reduce emissions (**Paper 1**, **Paper 2** and **Paper 3**).

It was observed that using HVO fuel instead of conventional diesel lowers both particulate and NO_x emissions with the engine applied in this thesis (**Paper 1**). This observation of emission reductions is in line with the previous HVO studies (Rantanen et al. 2005; Kuronen et al. 2007; Aatola et al. 2008; Murtonen et al. 2010). The properties of HVO emitted soot particles were studied in **Paper 4**. According to the results, the particles emitted using HVO were very similar to those emitted using conventional diesel both regarding their structure and their oxidation properties. The similarity of soot particles emitted with HVO to those emitted with conventional diesel is new information and it confirms that the existing aftertreatment technology is suitable for HVO-fueled engines.

The ability of HVO to decrease both particulate and NO_x emissions compared to conventional diesel arise most probably from the fact that HVO is practically free of aromatics. HVO also has much higher cetane number ($\approx$90) than conventional diesel ($\approx$50) which causes the engine adjustments designed for conventional diesel to be suboptimal for HVO fuel. The HVO fuel also provides an opportunity for more extensive use of NO_x reduction techniques due to the lower particulate emissions associated with the fuel. The chosen emissions reduction techniques studied in this thesis have not been previously applied to renewable fuels. In **Paper 1**, a variable valve timing strategy based on early inlet valve closing with constant inlet air mass flow (i.e. Miller timing) was tested with HVO fuel. The results indicated that, with HVO as fuel, the strategy showed potential to reduce NO_x emissions without considerable increases in particulate emissions. In **Paper 2**, the approach to use Miller timing with HVO fuel continued but, in this case, with the combined adjustments with EGR, injection pressure and injection timing. It was shown that particulate mass and NO_x

can both be reduced over 25 % by engine parameter adjustments. Further, the emission reductions were even higher when the engine parameter adjustments were targeted to reduce exclusively either particulates or NO_x. Nevertheless, it should be noted that the obtainable emission reductions depend strongly on the given engine and aftertreatment technology.

The other approach studied in this thesis to reduce exhaust emissions is the appliance of oxygenated HVO fuel. Oxygen in fuel reduces efficiently particulate emissions and, as HVO contains no oxygen, the addition of oxygenate could enable even higher particulate emission reductions. In **Paper 3**, a fuel blend containing 20 wt-% di-n-pentyl ether (DNPE) and wt-80 % HVO, thus having 2 wt-% oxygen content, was chosen as the oxygenated fuel. It was observed, that particulate emissions decreased over 25 % with the blend while NO_x emissions changed under 5 %. Thus, the use of oxygenate-HVO blend could provide even more clearance for the more pronounced reductions NO_x, for example, by using EGR. It was also observed, that the use of oxygenated HVO did not seem to significantly affect the properties of emitted particles regarding their hygroscopicity.

Time will tell what the role of HVO fuel is in the future. Currently, governments encourage the use of renewable fuels and, consequently, commercial production of HVO has increased considerably. Nevertheless, debates are still aroused whether the production of HVO fuel is environmentally sustainable or not. The greatest issue lies on the cultivation practices of the feedstock and, especially, on the land use changes associated with the cultivation. However, regardless of the outcome of these debates, this thesis has shown that HVO is technically a very attractive fuel. HVO reduces engine exhaust emissions while still being similar enough to conventional diesel so that the exhaust particle properties are not observably altered. There is also much potential to further reduce engine exhaust emissions with the fuel, for example, via engine optimization. Consequently, the fuel has potential to become one of the solutions that help to meet the increasingly strictening exhaust emission limits. Besides, it will not hurt to have another technology available to ease the next oil crisis.

References

Aatola, H., Larmi, M., Sarjovaara, T., Mikkonen, S., 2008. Hydrotreated vegetable oil (HVO) as a renewable diesel fuel: trade-off between NO_x, particulate emission, and fuel consumption of a heavy duty engine. SAE Technical Paper Series 2008-01-2500.

Abu-Jrai, A., Tsolakis, A., Theinnoi, K., Cracknell, R., Megaritis, A., Wyszynski, M. L., Golunski, S. E., 2006. Effect of gas-to-liquid diesel fuels on combustion characteristics, engine emissions, and exhaust gas fuel reforming. Comparative study. Energy & Fuels 20 (6), 2377–2384.

Armas, O., Yehliu, K., Boehman, A. L., 2010. Effect of alternative fuels on exhaust emissions during diesel engine operation with matched combustion phasing. Fuel 89 (2), 438–456.

Benajes, J., Molina, S., Martín, J., Novella, R., 2009a. Effect of advancing the closing angle of the intake valves on diffusion-controlled combustion in a HD diesel engine. Applied Thermal Engineering 29 (10), 1947–1954.

Benajes, J., Molina, S., Novella, R., Riesco, M., 2008. Improving pollutant emissions in diesel engines for heavy-duty transportation using retarded intake valve closing strategies. International Journal of Automotive Technology 9 (3), 257–265.

Benajes, J., Serrano, J. R., Molina, S., Novella, R., 2009b. Potential of Atkinson cycle combined with EGR for pollutant control in a HD diesel engine. Energy Conversion and Management 50 (1), 174–183.

Birch, M. E., Cary, R. A., 1996. Elemental carbon-based method for monitoring occupational exposures to particulate diesel exhaust. Aerosol Science and Technology 25 (3), 221–241.

Bunce, M., Snyder, D., Adi, G., Hall, C., Koehler, J., Davila, B., Kumar, S., Garimella, P., Stanton, D., Shaver, G., 2011. Optimization of soy-biodiesel combustion in a modern diesel engine. Fuel 90 (8), 2560–2570.

Chang, D. Y. Z., Van Gerpen, J. H., Lee, I., Johnson, L. A., Hammond, E. G., Marley, S. J., 1996. Fuel properties and emissions of soybean oil esters as diesel fuel. Journal of the American Oil Chemists' Society 73 (11), 1549–1555.

Cheng, Y. S., 2011. Condensation particle counters. In: Kulkarni, P., Baron, P. A., Willeke, K. (Eds.), Aerosol Measurement: Principles, Techniques and Applications, 3rd Edition. John Wiley & Sons, Inc., Ch. 17.

Demirbas, A., 2007a. Importance of biodiesel as transportation fuel. Energy Policy 35 (9), 4661–4670.

Demirbas, A., 2007b. Progress and recent trends in biofuels. Progress in Energy and Combustion Science 33 (1), 1–18.

Dieselnet, 2012. Automotive Diesel Fuel. `www.dieselnet.com/standards/eu/fuel_automotive.php#y1993`, [Online, Accessed March 20, 2012].

Dockery, D. W., Pope, C. A., Xu, X., Spengler, J. D., Ware, J. H., Fay, M. E., Ferris Jr, B. G., Speizer, F. E., 1993. An association between air pollution and mortality in six US cities. New England Journal of Medicine 329 (24), 1753–1759.

Dry, M. E., 2002. High quality diesel via the Fischer-Tropsch process – a review. Journal of Chemical Technology and Biotechnology 77 (1), 43–50.

Eastwood, P., 2008. Particulate emissions from vehicles. John Wiley & Sons.

EU, 2011. Commission Regulation (EU) No 582/2011 of 25 May 2011 implementing and amending Regulation (EC) No 595/2009 of the European Parliament and of the Council with respect to emissions from heavy duty vehicles (Euro VI) and amending Annexes I and III to Directive 2007/46/EC of the European Parliament and of the Council Text with EEA relevance. Official Journal of the European Union L 167, 1–168.

Fernando, S., Hall, C., Jha, S., 2006. NO_x reduction from biodiesel fuels. Energy & Fuels 20 (1), 376–382.

Filippo, A. D., Maricq, M. M., 2008. Diesel nucleation mode particles: semivolatile or solid? Environmental Science & Technology 42 (21), 7957–7962.

Giechaskiel, B., Ntziachristos, L., Samaras, Z., 2009. Effect of ejector dilutors on measurements of automotive exhaust gas aerosol size distributions. Measurement Science and Technology 20, 045703.

Gill, S. S., Tsolakis, A., Dearn, K. D., Rodríguez-Fernández, J., 2011a. Combustion characteristics and emissions of Fischer-Tropsch diesel fuels in IC engines. Progress in Energy and Combustion Science 37 (4), 503–523.

Gill, S. S., Tsolakis, A., Herreros, J. M., York, A. P. E., 2011b. Diesel emissions improvements through the use of biodiesel or oxygenated blending components. Fuel 95, 578–586.

Glaude, P., Fournet, R., Bounaceur, R., Molière, M., 2010. Adiabatic flame temperature from biofuels and fossil fuels and derived effect on NO_x emissions. Fuel Processing Technology 91 (2), 229–235.

Helwani, Z., Othman, M. R., Aziz, N., Fernando, W. J. N., Kim, J., 2009. Technologies for production of biodiesel focusing on green catalytic techniques: a review. Fuel Processing Technology 90 (12), 1502–1514.

Hennig, T., Massling, A., Brechtel, F. J., Wiedensohler, A., 2005. A tandem DMA for highly temperature-stabilized hygroscopic particle growth measurements between 90 % and 98 % relative humidity. Journal of Aerosol Science 36 (10), 1210–1223.

Henning, S., Ziese, M., Kiselev, A., Saathoff, H., Möhler, O., Mentel, T. F., Buchholz, A., Spindler, C., Michaud, V., Monier, M., Sellegri, K., Stratmann, F., 2012. Hygroscopic growth and droplet activation of soot particles: uncoated, succinic or sulfuric acid coated. Atmospheric Chemistry & Physics 12, 4525–4537.

Heywood, J. B., 1988. Internal combustion engine fundamentals. McGraw-Hill.

Higgins, K. J., Jung, H., Kittelson, D. B., Roberts, J. T., Zachariah, M. R., 2002. Size-selected nanoparticle chemistry: kinetics of soot oxidation. The Journal of Physical Chemistry A 106 (1), 96–103.

Higgins, K. J., Jung, H., Kittelson, D. B., Roberts, J. T., Zachariah, M. R., 2003. Kinetics of diesel nanoparticle oxidation. Environmental Science & Technology 37 (9), 1949–1954.

Hong, H., Parvate-Patil, G. B., Gordon, B., 2004. Review and analysis of variable valve timing strategies – eight ways to approach. Proceedings of the Institution of Mechanical Engineers. Part D: Journal of Automobile Engineering 218 (10), 1179–1200.

Huang, Y., Wang, S., Zhou, L., 2008. Effects of Fischer-Tropsch diesel fuel on combustion and emissions of direct injection diesel engine. Frontiers of Energy and Power Engineering in China 2 (3), 261–267.

Huber, G. W., Corma, A., 2007. Synergies between bio- and oil refineries for the production of fuels from biomass. Angewandte Chemie International Edition 46 (38), 7184–7201.

Ickes, A. M., Bohac, S. V., Assanis, D. N., 2009. Effect of fuel cetane number on a premixed diesel combustion mode. International Journal of Engine Research 10 (4), 251–263.

IEA, 2010. Key world energy statistics. International Energy Agency, Paris, `http://www.iea.org/textbase/nppdf/free/2010/key_stats_2010.pdf` [Online, Accessed July 21, 2012].

Imperato, M., Sarjovaara, T., Larmi, M., Kallio, I., Wik, C., 2010. Some experimental experience gained with a medium-speed diesel research engine. In: CIMAC Paper 238. Bergen, Norway, pp. 1–13.

Jain, S., Sharma, M. P., 2010. Prospects of biodiesel from jatropha in India: a review. Renewable and Sustainable Energy Reviews 14 (2), 763–771.

Johnson, G. R., Fletcher, C., Meyer, N., Modini, R., Ristovski, Z. D., 2008. A robust, portable H-TDMA for field use. Journal of Aerosol Science 39 (10), 850–861.

Joutsensaari, J., Vaattovaara, P., Vesterinen, M., Hämeri, K., Laaksonen, A., 2001. A novel tandem differential mobility analyzer with organic vapor treatment of aerosol particles. Atmospheric Chemistry and Physics 1 (1), 51–60.

Jung, H., Kittelson, D. B., Zachariah, M. R., 2006. Characteristics of SME biodiesel-fueled diesel particle emissions and the kinetics of oxidation. Environmental Science & Technology 40 (16), 4949–4955.

Kalam, M. A., Masjuki, H. H., 2002. Biodiesel from palmoil – an analysis of its properties and potential. Biomass and Bioenergy 23 (6), 471–479.

Keskinen, J., Pietarinen, K., Lehtimäki, M., 1992. Electrical low pressure impactor. Journal of Aerosol Science 23 (4), 353–360.

Kidoguchi, Y., Yang, C., Kato, R., Miwa, K., 2000. Effects of fuel cetane number and aromatics on combustion process and emissions of a direct-injection diesel engine. JSAE Review 21 (4), 469–475.

Kim, S. H., Woo, K. S., Liu, B. Y. H., Zachariah, M. R., 2005. Method of measuring charge distribution of nanosized aerosols. Journal of Colloid and Interface Science 282 (1), 46–57.

Kitamura, T., Ito, T., Senda, J., Fujimoto, H., 2001. Extraction of the suppression effects of oxygenated fuels on soot formation using a detailed chemical kinetic model. JSAE Review 22 (2), 139–145.

Kittelson, D. B., 1998. Engines and nanoparticles: a review. Journal of Aerosol Science 29 (5–6), 575–588.

Knauer, M., Carrara, M., Rothe, D., Niessner, R., Ivleva, N. P., 2008. Changes in structure and reactivity of soot during oxidation and gasification by oxygen, studied by micro-Raman spectroscopy and temperature programmed oxidation. Aerosol Science and Technology 43 (1), 1–8.

Knothe, G., Van Gerpen, J. H., Krahl, J., 2005. The biodiesel handbook. American Oil Chemists' Society.

Konstandopoulos, A. G., Kostoglou, M., 2000. Reciprocating flow regeneration of soot filters. Combustion and Flame 121 (3), 488–500.

Körbitz, W., 1999. Biodiesel production in Europe and North America, an encouraging prospect. Renewable Energy 16 (1–4), 1078–1083.

Kuronen, M., Mikkonen, S., Aakko, P., Murtonen, T., 2007. Hydrotreated vegetable oil as fuel for heavy duty diesel engines. SAE Technical Paper Series 2007-01-4031.

Labeckas, G., Slavinskas, S., 2006. The effect of rapeseed oil methyl ester on direct injection diesel engine performance and exhaust emissions. Energy Conversion and Management 47 (13), 1954–1967.

Laden, F., Schwartz, J., Speizer, F. E., Dockery, D. W., 2006. Reduction in fine particulate air pollution and mortality. American Journal of Respiratory and Critical Care Medicine 173 (6), 667–672.

Lähde, T., Rönkko, T., Happonen, M., Söderström, C., Virtanen, A., Solla, A., Kytö, M., Rothe, D., Keskinen, J., 2011. Effect of fuel injection pressure on a heavy-duty diesel engine nonvolatile particle emission. Environmental Science and Technology 45 (6), 2504–2509.

Lähde, T., Rönkkö, T., Virtanen, A., Schuck, T. J., Pirjola, L., Hämeri, K., Kulmala, M., Arnold, F., Rothe, D., Keskinen, J., 2008. Heavy duty diesel engine exhaust aerosol particle and ion measurements. Environmental Science & Technology 43 (1), 163–168.

Lancefield, T., Methley, I., Räse, U., Kuhn, T., 2000. The application of variable event valve timing to a modern diesel engine. SAE Technical Paper Series 2000-01-1229.

Lapuerta, M., Armas, O., Rodríguez-Fernández, J., 2008. Effect of biodiesel fuels on diesel engine emissions. Progress in Energy and Combustion Science 34 (2), 198–223.

Lapuerta, M., Oliva, F., Agudelo, J. R., Boehman, A. L., 2012. Effect of fuel on the soot nanostructure and consequences on loading and regeneration of diesel particulate filters. Combustion and Flame 159 (2), 844–853.

Lapuerta, M., Villajos, M., Agudelo, J. R., Boehman, A. L., 2011. Key properties and blending strategies of hydrotreated vegetable oil as biofuel for diesel engines. Fuel Processing Technology 92 (12), 2406–2411.

Le Treut, H., Somerville, R., Cubasch, U., Ding, Y., Mauritzen, C., Mokssit, A., Peterson, T., Prather, M., 2007. Historical overview of climate change. In: Solomon, S., Qin, D., Manning, M., Chen, Z., Marquis, M., Averyt, K. B., Tignor, M., Miller, H. L. (Eds.), Climate change 2007: the physical science basis. Contribution of Working Group I to the fourth assessment report of the intergovernmental panel on climate change.

Leung, D. Y. C., Luo, Y., Chan, T. L., 2006. Optimization of exhaust emissions of a diesel engine fuelled with biodiesel. Energy & Fuels 20 (3), 1015–1023.

Liu, B. Y. H., Pui, D. Y. H., Whitby, K. T., Kittelson, D. B., Kousaka, Y., McKenzie, R. L., 1978. The aerosol mobility chromatograph: a new detector for sulfuric acid aerosols. Atmospheric Environment 12 (1), 99–104.

Lyyränen, J., Jokiniemi, J., Kauppinen, E., Backman, U., Vesala, H., 2004. Comparison of different dilution methods for measuring diesel particle emissions. Aerosol Science and Technology 38 (1), 12–23.

Marchionna, M., Patrini, R., Giavazzi, F., Garibaldi, P., 2000. High cetane ethers for the reformulation of diesel fuels. In: 16th World Petroleum Congress. Calgary, Canada, pp. 38–45.

Maricq, M. M., Podsiadlik, D. H., Brehob, D. D., Haghgooie, M., 1999. Particulate emissions from a direct-injection spark-ignition (DISI) engine. SAE Technical Paper Series 1999-01-1530.

Martin, B., Aakko, P., Beckman, D., Del Giacomo, N., Giavazzi, F., 1997. Influence of future fuel formulations on diesel engine emissions – a joint European study. SAE Technical Paper Series 972966.

McCormick, R. L., Ross, J. D., Graboski, M. S., 1997. Effect of several oxygenates on regulated emissions from heavy-duty diesel engines. Environmental Science and Technology 31 (4), 1144–1150.

Mikkanen, P., Moisio, M., Keskinen, J., Ristimäki, J., Marjamäki, M., 2001. Sampling method for particle measurements of vehicle exhaust. SAE Technical Paper Series 2001-01-0219.

Miller, K. A., Siscovick, D. S., Sheppard, L., Shepherd, K., Sullivan, J. H., Anderson, G. L., Kaufman, J. D., 2007. Long-term exposure to air pollution and incidence of cardiovascular events in women. New England Journal of Medicine 356 (5), 447–458.

Miller, R. H., 1947. Supercharging and internal cooling cycle for high output. ASME Transactions 69, 453–457.

Mills, N., Donaldson, K., Hadoke, P., Boon, N., MacNee, W., Cassee, F., Sandström, T., Blomberg, A., Newby, D., 2008. Adverse cardiovascular effects of air pollution. Nature Clinical Practice Cardiovascular Medicine 6 (1), 36–44.

Müller, J. O., Su, D. S., Jentoft, R. E., Kröhnert, J., Jentoft, F. C., Schlögl, R., 2005. Morphology-controlled reactivity of carbonaceous materials towards oxidation. Catalysis Today 102, 259–265.

Murphy, M. J., 1999. Safety and industrial hygiene issues related to the use of oxygenates in diesel fuel. SAE Technical Paper Series 1999-01-1473.

Murphy, M. J., 2002. Oxygenate compatibility with diesel fuels. SAE Technical Paper Series 2002-01-2848.

Murray, J., King, D., 2012. Oil's tipping point has passed. Nature 481 (7382), 433–435.

Murtonen, T., Aakko-Saksa, P., Kuronen, M., Mikkonen, S., Lehtoranta, K., 2010. Emissions with heavy-duty diesel engines and vehicles using FAME, HVO and GTL fuels with and without DOC+POC aftertreatment. SAE International Journal of Fuels and Lubricants 2 (2), 147–166.

Nabi, M., Hustad, J., 2010. Influence of biodiesel addition to Fischer-Tropsch fuel on diesel engine performance and exhaust emissions. Energy & Fuels 24 (5), 2868–2874.

Neeft, J., Makkee, M., Moulijn, J. A., 1996. Diesel particulate emission control. Fuel Processing Technology 47 (1), 1–69.

Ntziachristos, L., Giechaskiel, B., Pistikopoulos, P., Samaras, Z., Mathis, U., Mohr, M., Ristimäki, J., Keskinen, J., Mikkanen, P., Casati, R., et al., 2004. Performance evaluation of a novel sampling and measurement system for exhaust particle characterization. SAE Technical Paper Series 2004-01-1439.

Oberdörster, G., Sharp, Z., Atudorei, V., Elder, A., Gelein, R., Kreyling, W., Cox, C., 2004. Translocation of inhaled ultrafine particles to the brain. Inhalation toxicology 16 (6-7), 437–445.

Pachauri, R. K., Reisinger, A. (Eds.), 2007. Climate Change 2007: Synthesis Report. Contribution of Working Groups I, II and III to the Fourth Assessment Report of the Intergovernmental Panel on Climate Change. IPCC.

Pecci, G. C., Clerici, M. G., Giavazzi, F., Ancillotti, F., Marchionna, M., Patrini, R., 1991. Oxygenated diesel fuels. Part I – structure and properties correlation. In: Proceedings of the 9th International Symposium on Alcohol Fuels (ISAF). Firenze, Italy, pp. 321–326.

Pope III, C. A., Ezzati, M., Dockery, D. W., 2009. Fine-particulate air pollution and life expectancy in the United States. New England Journal of Medicine 360 (4), 376–386.

Rader, D. J., McMurry, P. H., 1986. Application of the tandem differential mobility analyzer to studies of droplet growth or evaporation. Journal of Aerosol Science 17 (5), 771–787.

Rantanen, L., Linnaila, R., Aakko, P., Harju, T., 2005. NExBTL – biodiesel fuel of the second generation. SAE Technical Paper Series 2005-01-3771.

Ren, Y., Huang, Z., Miao, H., Di, Y., Jiang, D., Zeng, K., Liu, B., Wang, X., 2008. Combustion and emissions of a DI diesel engine fuelled with diesel-oxygenate blends. Fuel 87 (12), 2691–2697.

Rönkkö, T., Virtanen, A., Kannosto, J., Keskinen, J., Lappi, M., Pirjola, L., 2007. Nucleation mode particles with a nonvolatile core in the exhaust of a heavy duty diesel vehicle. Environmental Science & Technology 41 (18), 6384–6389.

Rönkkö, T., Virtanen, A., Vaaraslahti, K., Keskinen, J., Pirjola, L., Lappi, M., 2006. Effect of dilution conditions and driving parameters on nucleation mode particles in diesel exhaust: laboratory and on-road study. Atmospheric Environment 40 (16), 2893–2901.

Satoh, K., Zhang, L., Hatanaka, H., Takatsuki, T., Yokota, K., 1997. Relationship between NO_x and SM emissions from DI diesel engine with EGR. JSAE Review 18 (4), 369–375.

Semelsberger, T. A., Borup, R. L., Greene, H. L., 2006. Dimethyl ether (DME) as an alternative fuel. Journal of Power Sources 156 (2), 497–511.

Shrivastava, M., Nguyen, A., Zheng, Z., Wu, H. W., Jung, H. S., 2010. Kinetics of soot oxidation by NO_2. Environmental Science & Technology 44 (12), 4796–4801.

Sorenson, S. C., 2001. Dimethyl ether in diesel engines: progress and perspectives. Journal of Engineering for Gas Turbines and Power 123 (3), 652–658.

Su, D., Jentoft, R., Müller, J., Rothe, D., Jacob, E., Simpson, C., Tomović, Ž., Müllen, K., Messerer, A., Pöschl, U., et al., 2004a. Microstructure and oxidation behaviour of Euro IV diesel engine soot: a comparative study with synthetic model soot substances. Catalysis Today 90 (1), 127–132.

Su, D. S., Müller, J. O., Jentoft, R. E., Rothe, D., Jacob, E., Schlögl, R., 2004b. Fullerene-like soot from Euro IV diesel engine: consequences for catalytic automotive pollution control. Topics in Catalysis 30 (1), 241–245.

Su, D. S., Serafino, A., Müller, J. O., Jentoft, R. E., Schlögl, R., Fiorito, S., 2008. Cytotoxicity and inflammatory potential of soot particles of low-emission diesel engines. Environmental Science & Technology 42 (5), 1761–1765.

Sunde, K., Brekke, A., Solberg, B., 2011. Environmental impacts and costs of hydrotreated vegetable oils, transesterified lipids and woody BTL – a review. Energies 4 (6), 845–877.

Tijmensen, M. J. A., Faaij, A. P. C., Hamelinck, C. N., van Hardeveld, M. R. M., 2002. Exploration of the possibilities for production of Fischer-Tropsch liquids and power via biomass gasification. Biomass and Bioenergy 23 (2), 129–152.

Tilli, A., Imperato, M., Aakko-Saksa, P., Larmi, M., Sarjovaara, T., Honkanen, M., 2010. High cetane number paraffinic diesel fuels and emission reduction in engine combustion. In: CIMAC Paper 26. Bergen, Norway, pp. 1–14.

Vaaraslahti, K., Virtanen, A., Ristimäki, J., Keskinen, J., 2004. Nucleation mode formation in heavy-duty diesel exhaust with and without a particulate filter. Environmental Science & Technology 38 (18), 4884–4890.

Vander Wal, R. L., Tomasek, A. J., 2003. Soot oxidation: dependence upon initial nanostructure. Combustion and Flame 134 (1-2), 1–9.

Vander Wal, R. L., Tomasek, A. J., Street, K., Hull, D. R., Thompson, W. K., 2004. Carbon nanostructure examined by lattice fringe analysis of high-resolution transmission electron microscopy images. Applied Spectroscopy 58 (2), 230–237.

Wang, S. C., Flagan, R. C., 1990. Scanning electrical mobility spectrometer. Aerosol Science and Technology 13 (2), 230–240.

Wang, X., Cheung, C. S., Di, Y., Huang, Z., 2012. Diesel engine gaseous and particle emissions fueled with diesel–oxygenate blends. Fuel 94, 317–323.

Wang, Y., Zeng, S., Huang, J., He, Y., Huang, X., Lin, L., Li, S., 2005. Experimental investigation of applying Miller cycle to reduce NO_x emission from diesel engine. Proceedings of the Institution of Mechanical Engineers, Part A: Journal of Power and Energy 219 (8), 631–638.

Weingartner, E., Burtscher, H., Baltensperger, U., 1997. Hygroscopic properties of carbon and diesel soot particles. Atmospheric Environment 31 (15), 2311–2327.

Weingartner, E., Gysel, M., Baltensperger, U., 2002. Hygroscopicity of aerosol particles at low temperatures. 1. New low-temperature H-TDMA instrument: setup and first applications. Environmental Science & Technology 36 (1), 55–62.

WHO, 2012. IARC: diesel engine exhaust carsinogenic. `http://press.iarc.fr/pr213_E.pdf`, press release 12 June 2012, [Online, Accessed July 9, 2012].

Williams, D. B., Carter, C. B., 2009. Transmission Electron Microscopy. A Textbook for Materials Science. Springer.

Wu, T., Huang, Z., Zhang, W., Fang, J., Yin, Q., 2007. Physical and chemical properties of GTL-diesel fuel blends and their effects on performance and emissions of a multicylinder DI compression ignition engine. Energy & Fuels 21 (4), 1908–1914.

Xi, J., Zhong, B. J., 2006. Soot in diesel combustion systems. Chemical Engineering & Technology 29 (6), 665–673.

Zheng, M., Reader, G. T., Hawley, J. G., 2004. Diesel engine exhaust gas recirculation – a review on advanced and novel concepts. Energy Conversion and Management 45 (6), 883–900.

Tampereen teknillinen yliopisto
PL 527
33101 Tampere

Tampere University of Technology
P.O.B. 527
FI-33101 Tampere, Finland

ISBN 978-952-15-2921-4
ISSN 1459-2045